

Enhancing Quantum Algorithms for Quadratic Unconstrained Binary Optimization via Integer Programming

Friedrich Wagner ^{*} Jonas Nüßlein [†] Frauke Liers [‡]

29th April 2024

Abstract

To date, research in quantum computation promises potential for outperforming classical heuristics in combinatorial optimization. However, when aiming at provable optimality, one has to rely on classical exact methods like integer programming. State-of-the-art integer programming algorithms can compute strong relaxation bounds even for hard instances, but may have to enumerate a large number of subproblems for determining an optimum solution. If the potential of quantum computing realizes, it can be expected that in particular finding high-quality solutions for hard problems can be done fast. Still, near-future quantum hardware considerably limits the size of treatable problems. In this work, we go one step into integrating the potentials of quantum and classical techniques for combinatorial optimization. We propose a hybrid heuristic for the weighted maximum-cut problem or, equivalently, for quadratic unconstrained binary optimization. The heuristic employs a linear programming relaxation, rendering it well-suited for integration into exact branch-and-cut algorithms. For large instances, we reduce the problem size according to a linear relaxation such that the reduced problem can be handled by quantum machines of limited size. Moreover, we improve the applicability of QAOA, a parameterized quantum algorithm, by deriving optimal parameters for special instances which motivates a parameter estimate for arbitrary instances. We present numerous computational results from real quantum hardware.

Keywords: Integer Programming, Combinatorial Optimization, Quantum Computation

1 Introduction

Mixed-integer programming looks back upon a long history of successfully developing methods and algorithms. Although being NP-hard, algorithmic enhancements have led to the result that even difficult instances can be solved to global optimality, often quickly, by modern algorithms and implementations, [1, 2, 3]. Nonetheless, there exist practically relevant instances which exceed the capabilities of state-of-the-art solvers [4]. On the other hand, recent progress in quantum computation promises fast, high-quality heuristics for such problems [5, 6]. Important examples for such heuristics are quantum annealing [7, 8] and the quantum approximate optimization algorithm (QAOA) [9, 10]. Although it is unclear whether this promise will realize and near-future quantum hardware strongly limits the size of treatable problems [11, 12, 13], quantum computation is a highly relevant topic that is currently studied in many research groups.

In this work, we take a step towards combining the potential of quantum and classical computation, with the goal of enhancing the applicability of quantum algorithms such that larger instances can be solved. We propose a hybrid, heuristic algorithm for the weighted maximum-cut problem (MaxCut). The algorithm builds on a well-known linear relaxation of MaxCut. Solving linear

^{*}Fraunhofer Institute for Integrated Circuits IIS, Erlangen, Germany,
Department of Data Science, University of Erlangen-Nuremberg, Germany, friedrich.wagner@iis.fraunhofer.de

[†]Department of Data Science, University of Erlangen-Nuremberg, Germany

[‡]Department of Data Science, University of Erlangen-Nuremberg, Germany

relaxations is the basis of branch-and-cut algorithms for integer programming since they provide upper bounds on an optimum solution value (we consider here the case of a maximization problem). Branch-and-cut divides the solution space into subproblems, called *branching*, and calculates upper bounds on the best solution value in each subproblem by solving a linear relaxation. If this upper bound undercuts the best known lower bound, typically given by the value of the best available solution, the subproblem can be pruned, i.e. excluded entirely from the search. Otherwise, the algorithm continues branching. Linear relaxations can be often solved quickly, even for very large instances [3]. Thus, the proposed heuristic is particularly well-suited for integration in integer programming methods. Integrating fast and high-quality heuristics in classical branch-and-cut is a commonly used technique to speed up the solution process [14]. Such heuristics provide quickly accessible lower bounds. If there is a gap between upper and lower bound, the algorithm needs to branch and starts enumerating sub-problems. The need to enumerate a large number of sub-problems often slows down the solution process significantly. Branch-and-cut performs particularly well when upper and lower bounds are strong as branching can then be avoided as much as possible. Heuristics based on linear relaxation solutions are implemented in all state-of-the-art solvers for integer programming. Typically, they perform an elaborate rounding procedure to derive feasible integer solutions [15]. In this work, we solve the so-called *cycle relaxation* of MaxCut, which has proven valuable for rounding heuristics in previous works [16, 17, 18]. However, we emphasize that *any* relaxation can readily be substituted in our method. The proposed heuristics fixes variables based on rounding a cycle relaxation solution. Together with careful algorithm engineering, this allows to shrink the problem size to a specified target value such that it can be handled by quantum hardware of limited size. Thus, instead of relying on branching to determine an integer solution, the enumerative part is heuristically solved by quantum computation. Finally, having retrieved a solution to the reduced problem from the quantum algorithm, a solution to the original MaxCut instance is recovered by undoing the shrinking operations appropriately. This procedure combines the advantages of integer programming, i.e. the ability to solve large relaxations, with the advantages of quantum computation, i.e. the ability to determine high-quality solutions quickly.

However, current quantum algorithms for combinatorial optimization are typically parameterized and parameters need to be tuned in a feedback-loop in order to retrieve satisfactory results. This heavily increases runtime which would render such quantum heuristics impractical for integration into integer programming solvers. To tackle this issue, we develop a method to derive good parameters efficiently for QAOA in the case of weighted MaxCut, speeding up the quantum part of the proposed method by several orders of magnitude. The proposed method benefits from decades of developing linear programming techniques for MaxCut which we briefly summarize here.

Linear programming and MaxCut. Given a weighted graph, MaxCut asks for a partition of the nodes such that the weight of connecting edges is maximized. The decision version of MaxCut is one of Karp’s 21 NP-complete problems [19]. Thus, polynomial time algorithms are known for special cases only, e.g. for planar graphs [20, 21], for graphs without long odd cycles [22] and for graphs with no K_5 minor [23]. The work of Barahona and Mahjoub [23] paved the way for a long series of successful applications of linear programming (LP) methods for MaxCut. For a comprehensive book, we refer the interested reader to [24]. A major reason for this success is the development of sophisticated techniques that allow the solution of large LP relaxations of MaxCut, cf. e.g. [25, 18, 26, 27]. From a theoretical point of view, these linear relaxations have a rather large worst-case integrality gap of 2 [28, 29].¹ In practice, however, they are typically much stronger, i.e. they yield a tight upper bound on the optimum cut value, making them valuable for branch-and-cut algorithms, cf. [16, 25, 17, 30, 31]. For LP based methods, it is well-known that the difficulty of solving MaxCut instances to global optimality strongly depends on the density of the underlying graph. Indeed, dense instances in the order of 100 vertices can already go beyond what is solvable in practice by modern algorithms. However, if instances are sparse and possibly defined on regular structures such as grid graphs, or if the weights are specifically designed, state-of-the-art methods can handle problems with over 10,000 vertices in less than a minute, cf. [31].

¹Here, the integrality gap of a relaxation is defined as the relaxation optimum value divided by an optimum integer solution value.

Another widespread relaxation of MaxCut is based on semi-definite programming (SDP). It was first introduced by Goemans and Williamson [32] who developed a famous α -approximation algorithm for MaxCut with $\alpha \approx 0.878$. Indeed, it was shown later that α is the best possible approximation factor for a polynomial-time algorithm if the Unique Games Conjecture holds [33]. Moreover, the integrality gap of the SDP-relaxation is precisely $1/\alpha \approx 1.14$ [34], which is considerably smaller than the integrality gap of LP relaxations. In practice, SDP based exact algorithms perform well even on dense instances, contrary to LP-methods. However, they scale (much) worse than LP-methods w.r.t. to the number of vertices, cf. [35, 36, 37]. Noteworthy, strong relaxations of MaxCut have proven useful even for problems with additional constraints [38].

Quantum computation and MaxCut. Significant technological progress in quantum computation (QC) hardware has been achieved in the last decade, improving both digital (cf. e.g. [39, 40]) and analog quantum computers (cf. e.g. [41, 42]). The availability of quantum hardware has driven researchers to seek for practical quantum advantage in various fields of applications. Among those, combinatorial optimization plays a prominent role (cf. e.g. [6]), although clear advantages have not yet been shown [43, 12]. Here, commonly used algorithms are the QAOA in digital QC (cf. [9]), and quantum annealing in analog QC (cf. [41]). Although from a theoretical point of view, both algorithms are applicable to a broad range of combinatorial optimization problems, research is mainly focused on quadratic unconstrained binary optimization (QUBO). QUBO and MaxCut are equivalent problems as there exists a linear transformation between them. In particular, any QUBO problem on n variables can be transformed into an equivalent MaxCut instance on $n + 1$ vertices (cf. [44, 25, 45]). We detail this transformation in Sec. 3. The reason for the prominence of QUBO in QC is that many current quantum hardware platforms, both digital and analog, have a natural connection to QUBO.² Therefore, the usual approach is to model the problem of interest as a QUBO problem [46]. Moreover, technical restrictions of current hardware limit the size of treatable QUBO problems. The maximum treatable problem size depends not only on the hardware size but also heavily on the problem density. Here, analog QC encounters significant overhead in quantum resources when embedding dense problem graphs onto sparse hardware graphs [47, 48]. Similarly, in digital QC, qubit routing adds additional quantum overhead for dense problems [49]. In digital QC, also error correction [50] or error mitigation [51, 52] require additional resources. It is reasonable to expect that, even if QC achieves clear experimental advantages, such restrictions due to quantum hardware persist. Therefore, algorithmic size-reduction techniques will be necessary to leverage the full potential of QC.

Our contribution. In this work, we present a novel hybrid quantum-classical heuristic for MaxCut which can easily be integrated into modern integer programming solvers. The proposed algorithm overcomes the limitations of near-future quantum hardware by employing classical size-reduction techniques. In the context of classical algorithms, our main contribution is the combination of graph shrinking with linear programming. This allows to combine the advantages of both quantum and classical methods for combinatorial optimization: The former can be expected to quickly produce high-quality solutions for hard instances (cf. e.g. [53, 54, 55]) but the size of treatable problems is limited. The latter can efficiently compute strong relaxations, in particular on sparse instances of large size [31].

Additionally, we improve the applicability of the quantum algorithm used in our experiments – QAOA for weighted MaxCut – by deriving optimal parameters for triangle-free, regular graphs with weights following a binary distribution. To this end, we derive an alternate formula for the expectation value of depth-1 QAOA applied to weighted MaxCut by extending the work of [56]. This formula is less expensive to evaluate numerically than the formula derived in Refs. [57, 53] on sparse instances. Furthermore, this leads a new estimate for good parameter values for arbitrary instances. As a result, the runtime of the quantum algorithm is reduced, which is especially beneficial when integrating it into classical branch-and-cut.

We present various experimental results from quantum simulators and real quantum hardware, showing the applicability of the proposed method on example instances inspired by spin glass

²In the physics literature, usually the term “Ising model” is used instead of QUBO.

physics. The quantum processor in our experiments has 27 qubits of which we use at most 10 due to strong noise. This limits the size of the reduced problem to a maximum of 10 vertices. Due to the hybrid algorithm that first reduces the instance size classically, we solve instances with up to 100 vertices within 60 s of total computation time, including classical runtime and runtime on real quantum hardware. For standard QAOA without classical size reduction, these instances exceed the currently available resources. We emphasize, that all instances considered in this work can be solved in reasonable time by purely classical methods. Owing to the limited size of the quantum hardware used in this work, larger instances would not give deeper insights in the quantum part since the algorithm outcome would mainly be determined by the classical part. Our experiments thus yield a proof-of-principle, encouraging the application of the proposed method when quantum hardware advances.

Structure. The remainder of this paper is organized as follows: First, we give an overview of and discuss connections to related literature in Section 2. In Section 3, we formally introduce the MaxCut and QUBO problem as well as QAOA. Section 4 describes our algorithm in detail. In Section 5, we derive the novel result on optimum QAOA-parameters. Section 6 presents various experimental results. We conclude with a summary and indicate further directions of research in Section 7.

2 Related work

In the context of QAOA, a similar size-reduction procedure, known as *recursive QAOA* (RQAOA), has been proposed in [53] and was further developed in [58, 59]. In those works, however, the motivation is quite different. The authors reduce large-scale problems by iteratively solving them approximately by QC in order to reach regimes where classical exact methods can be applied. While their size-reduction technique is similar to ours, they use QC to determine the next reduction step. Thus, for practical applicability, large-scale quantum hardware would be required. This is also the case for the algorithm proposed in [60] which employs variable correlations generated by QAOA in order to obtain valid QUBO solutions via a rounding procedure.

The authors of [61] and [62] combine classical semi-definite relaxations of MaxCut with QAOA. They employ relaxation solutions for warm-starting QAOA in order to achieve better results. On the contrary, in this work, relaxation solutions are used to reduce problem size. Furthermore, in the context of QA, size-reduction was successfully applied in [63]. There, the problem size is reduced – similarly to this work – by fixing a set of variables. The authors repetitively choose a random set of variables to be fixed and try to improve an overall solution by solving the reduced problem via QA. This is in contrast to this work, where the set of variables to be fixed is determined by a relaxation solution.

The performance of QAOA for MaxCut was studied by the authors of [13] and [11]. Their results indicate a high threshold for QAOA to achieve an advantage over classical heuristics. However, their study is restricted to unweighted 3-regular graphs, whereas our work deals with arbitrary, weighted graphs.

The authors of [57] derive an analytical expressions for the expectation value produced by depth-1 QAOA on general Ising models, which includes weighted MaxCut. The same analytical expression for weighted MaxCut was already obtained in [53]. In this work, we derive a different formula for weighted MaxCut by extending a result on unweighted MaxCut from [56] and [64]. The resulting, alternative formula is cheaper to evaluate than the formula from [57] and [53] for sparse instances.

Moreover, the authors of [57] derive parameters which are optimal on regular graphs in the ensemble average for normally distributed weights. Similarly, Ref. [54] gives an explicit formula for the ensemble average of the expectation value for arbitrary-depth QAOA applied to the Sherrington-Kirkpatrick model of infinite size. Therein, the authors derive optimal parameters for the depth-1 case. In contrast, in this work we derive (approximate) optimal parameters for a given instance rather than averaging over an instance ensemble. Furthermore, deducing high-quality QAOA-parameters for weighted MaxCut was studied in [65]. There, the authors successfully transfer

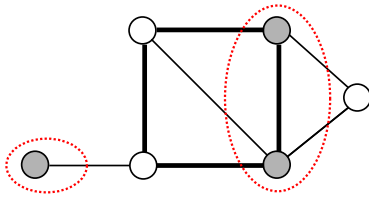


Figure 1: Example for a cut. A vertex subset W is marked in gray. All edges crossed by the red dashed lines are in the cut $\delta(W)$. An exemplary cycle of length four is marked by thick edges. It intersects with the red dashed line two times. In general, any cycle intersects with $\delta(W)$ an even number of times.

parameters which are known to be well-suited for unweighted MaxCut to the weighted case. On the contrary, the method for QAOA-parameter estimation proposed in this work is purely based on characteristics of the weighted MaxCut instance at hand.

Fixing variables in order to reduce the problem size is an established pre-processing technique in integer programming algorithms. Here, one seeks for variable assignments that are provably part of an optimum solution since then solving the reduced problem will recover an optimum solution to the original instance. For MaxCut, such methods are developed in e.g. [66, 67, 30]. Clearly, an advantage of such techniques is that it allows to reduce the problem size without losing the possibility to retrieve an optimum solution. On the other hand, they are computationally more expensive than rounding relaxation solutions and reaching a specific target size of the reduced problem cannot be ensured. This, however, is crucial in the context of this work since quantum hardware strictly limits the size of treatable problems.

Considering heuristics for integer programming, rounding variables according to a relaxation solution is a commonly used paradigm. In the context of MaxCut, it was already applied in the early work of Barahona et al. [16] and, more recently, e.g. in [17, 18]. In those works, a set of variables corresponding to a spanning tree is rounded, as this uniquely defines a cut. The spanning tree is chosen such that its variables are as close to integer as possible. Computationally, this can be implemented efficiently by a minimum-weight spanning-tree algorithm. In this work, however, only a subset of variables (which corresponds to a forest) is fixed by rounding, leaving the remaining variables free to be optimized by the quantum algorithm. Furthermore, shrinking was successfully applied to other closely related combinatorial optimization problems in [22, 68].

3 Preliminaries

Before stating our results, we introduce the prerequisites necessary for the upcoming sections. First, we formally define the MaxCut problem and introduce its integer programming model. Then, we define the QUBO problem and recap the transformation between QUBO and MaxCut. Finally, we introduce QAOA and its application to MaxCut.

MaxCut and QUBO As stated earlier, MaxCut and QUBO are well known to be equivalent problems. For ease of presentation, we introduce the maximum cut problem first as this is natural for integer programming methods. Given an undirected graph $G = (V, E)$ and a vertex subset $W \subseteq V$, the edge set $\delta(W) := \{uv \in E \mid u \in W, v \notin W\}$ is called a *cut* of G . For edge weights $w \in \mathbb{R}^{|E|}$, the weight of a cut $\delta(W)$ is defined as $\sum_{e \in \delta(W)} w_e$. The MaxCut problem asks for a cut of maximum weight. An edge subset $C = \{v_0v_1, v_1v_2, \dots, v_{k-1}v_k, v_kv_0\} \subseteq E$ is called a *cycle*. Clearly, a cut and a cycle always coincide in an even number of edges as illustrated in Fig. 1. Algebraically, this observation can be modeled by the so-called *odd-cycle inequalities* [23]. If C is a cycle and $x \in \{0, 1\}^{|E|}$ is the edge incidence-vector of a cut, it holds

$$\sum_{e \in Q} x_e - \sum_{e \in C \setminus Q} x_e \leq |Q| - 1 \quad \forall Q \subseteq C, |Q| \text{ odd.}$$

In fact, the odd-cycle inequalities for all cycles C are sufficient to define a cut. Thus, a widely used integer linear programming formulation (cf. e.g. [16, 25, 26, 30]) of MaxCut is

$$\max_x \sum_{e \in E} w_e x_e \quad (1a)$$

$$\text{s.t.} \quad \sum_{e \in Q} x_e - \sum_{e \in C \setminus Q} x_e \leq |Q| - 1 \quad \forall Q \subseteq C, |Q| \text{ odd}, \forall C \subseteq E \text{ cycle} \quad (1b)$$

$$0 \leq x_e \leq 1 \quad \forall e \in E \quad (1c)$$

$$x_e \in \{0, 1\} \quad \forall e \in E. \quad (1d)$$

The *cut polytope*, first introduced in [23], is the convex hull of all cut incidence-vectors,

$$P_{\text{CUT}} := \text{conv}\{x \in \mathbb{R}^{|E|} \mid (1b) - (1d)\}.$$

Dropping the integrality condition (1d), the model (1a)-(1c) is called the *cycle relaxation* of MaxCut. In general, a solution to the cycle relaxation yields an upper bound on the optimum cut value. However, it is known that the cycle relaxation has integer optimal solutions for all weights $w_e \in \mathbb{R}^{|E|}$ if and only if G has no K_5 minor, cf. [23]. Although the MaxCut problem is NP-hard, optimizing the cycle relaxation can be done in polynomial time via *odd-cycle separation*. First, only (1a) and (1c) is optimized. Given an optimal solution x^* , the odd-cycle separation algorithms decides whether x^* satisfies all odd-cycle inequalities. If not, it returns a violated one which is added to the model and the procedure is repeated. Otherwise, x^* is optimal for the cycle relaxation. Barahona and Majhoub [25] give a polynomial-time algorithm for odd-cycle separation based on shortest paths. Typically, one seeks for odd-cycle inequalities that belong to *chordless* cycles as they define facets of the cut polytope, cf. [23, 26]. For complete graphs, the odd-cycle inequalities take the form

$$x_{tu} - x_{uv} - x_{vt} \leq 0 \quad (2a)$$

$$-x_{tu} + x_{uv} - x_{vt} \leq 0 \quad (2b)$$

$$-x_{tu} - x_{uv} + x_{vt} \leq 0 \quad (2c)$$

$$x_{tu} + x_{uv} + x_{vt} \leq 2 \quad (2d)$$

for all triangles $\{t, u, v\}$ in G . A key ingredient of our algorithm is, that a solution to the cycle relaxation can be computed efficiently. We thus use an optimum cycle relaxation solution to reduce the size of the MaxCut instance such that it can be handled by near-term quantum computers. To this end, we identify an edge whose corresponding value of the relaxation solution is close to integer. Then, the two incident vertices are replaced by a single vertex. We refer to such a new vertex originating from replacing two vertices as a *super-vertex*. We repeat this vertex replacement until a target size is reached. This process is called *shrinking*, cf. [68, 18]. Details are explained in Section 4.

Current research in quantum computation for combinatorial optimization mainly focuses on QUBO problems, that is, problems of the form

$$\begin{aligned} \max_x \quad & \sum_{i,j} q_{ij} x_i x_j \\ \text{s.t.} \quad & x_i \in \{0, 1\} \quad \forall i \in \{1, \dots, n\}, \end{aligned}$$

where $q_{ij} \in \mathbb{R}$. A QUBO problem with n variables can be transformed to an equivalent MaxCut problem on $n + 1$ vertices, cf. [44, 25, 45, 27]. To this end, we consider the complete graph K_{n+1} with vertices $\{0, 1, \dots, n\}$. For an edge $ij \in K_{n+1}$ with $i, j > 0$, we define its weight as $w_{ij} = q_{ij} + q_{ji}$. Moreover, for an edge $i0$ with $i > 0$, we set $w_{i0} = \sum_{j=1}^n q_{ij} + q_{ji}$. Then, a cut $\delta(W)$ with weight W gives rise to a QUBO solution with value $Q = -W/2 + C$ where $C = 1/4 \left(\sum_{e \in E} w_e + 2 \sum_i q_{ii} + \sum_{i < j} q_{ij} + q_{ji} \right)$. The QUBO solution is obtained by setting $x_i = 0$ if $i0$ is in the cut $\delta(W)$ and $x_i = 1$ otherwise.

Our size-reduction method works on MaxCut, but we keep in mind that this MaxCut problem might originate from a transformed QUBO problem. After size-reduction, we formulate the reduced MaxCut problem as a QUBO problem in order to use QC for its solution. The natural QUBO formulation of MaxCut is

$$\max_x C(x) = \sum_{uv \in E} w_{uv}(x_u + x_v - 2x_u x_v) \quad (4a)$$

$$\text{s.t. } x_v \in \{0, 1\} \quad \forall v \in V. \quad (4b)$$

This model is then solved by QAOA and a solution to the original MaxCut (or QUBO) problem is reconstructed.

QAOA. QAOA is a quantum-classical hybrid algorithm, originally proposed by Fahri et al. in [9]. Since then, it has received great attention, which led to the development of more sophisticated versions and variants, see e.g. [53, 69]. QAOA computes approximate solutions of arbitrary, unconstrained, binary optimization problems defined by a target function $C : \{0, 1\}^n \rightarrow \mathbb{R}$. The goal is to find an $x^* \in \{0, 1\}^n$ maximizing the target function. QAOA is a parameterized algorithm with real-valued parameters $\gamma = (\gamma_1, \dots, \gamma_p)$ and $\beta = (\beta_1, \dots, \beta_p)$. The hyper-parameter p , called *depth*, controls the computational complexity of the algorithm. QAOA prepares the quantum state

$$|\psi(\beta, \gamma)\rangle = e^{-i\beta_p H_M} e^{-i\gamma_p H_C} \dots e^{-i\beta_1 H_M} e^{-i\gamma_1 H_C} |+\rangle.$$

Here, H_C is the problem-specific *phase Hamiltonian*, defined by

$$H_C |x\rangle = C(x) |x\rangle \quad \forall x \in \{0, 1\}^n \quad (5)$$

and H_M is the problem-independent *mixing Hamiltonian*, defined by

$$H_M = \sum_{i=1}^n X_i,$$

where X_i is the Pauli X -operator acting on qubit i . The initial state $|+\rangle$ is the uniform superposition over all basis states, that is

$$|+\rangle = \frac{1}{\sqrt{2^n}} \sum_{x \in \{0, 1\}^n} |x\rangle.$$

Performing a single measurement yields a bit string x with probability $P_{\gamma, \beta}(x) = |\langle x | \psi(\beta, \gamma) \rangle|^2$. Thus, the expectation value of $C(x)$ evaluates to

$$F(\beta, \gamma) := \sum_{x \in \{0, 1\}^n} P_{\gamma, \beta}(x) C(x) = \langle \psi(\beta, \gamma) | H_C | \psi(\beta, \gamma) \rangle. \quad (6)$$

The distribution $P_{\gamma, \beta}(x)$ is parameter-dependent, and one seeks for parameters that yield high probabilities for high value solutions. Usually, this is done by classically maximizing the expectation value $F(\gamma, \beta)$ which is estimated by an average over a finite sample

$$\langle C \rangle(\gamma, \beta) = \frac{1}{N} \sum_{i=1}^N C(x_i), \quad (7)$$

where N is the total number of samples and $x_i \in \{0, 1\}^n$ is the i -th sample. We remark, that another, less common metric for parameter optimization is the probability of sampling an optimal solution. If the value of an optimum solution is unknown, as is typically the case for MaxCut, this metric is only applicable for small instances because it requires calculating the optimum solution value beforehand.

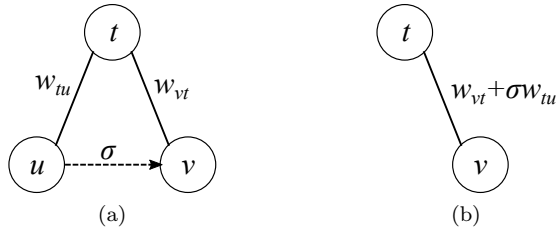


Figure 2: Sketch for vertex shrinking. (a): Vertices u and v are to be identified, where $\sigma \in \{-1, 1\}$ defines whether u and v lie in the equal or opposite partitions. Vertex t is a neighbor of u . (b): In the shrunk MaxCut instance, vertex v is a super-vertex containing u and v with adjusted edge weights. In the case where edge vt is not present in (a), it is constructed as shown in (b) with $w_{vt} = 0$.

In the experiments, we use QAOA for the weighted-MaxCut target-function given in (4a). It is easily verified, that the phase Hamiltonian

$$H_C = \sum_{uv \in E} \frac{w_{uv}}{2} (I - Z_u Z_v) \quad (8)$$

fulfils (5) for this particular target function. Here, Z_u is the Pauli Z -operator acting on qubit u . Having introduced the necessary prerequisites, we now describe the proposed quantum-classical algorithm in more detail.

4 Algorithm description

In this section, we describe the proposed hybrid algorithm for MaxCut problems. It can be divided into four major steps. First, *correlations* between vertex pairs are computed from an optimum cycle relaxation solution. Here, the closeness of a relaxation variable to an integer value is interpreted as a tendency of the corresponding vertex pair to lie in equal or opposite partitions in an optimum cut. Second, the problem size is reduced by imposing correlations, that is, vertex pairs with large absolute correlations are identified. Third, the shrunk problem is solved by QAOA. Finally, a feasible solution to the original problem is reconstructed by undoing the shrinking operations appropriately.

Computing Correlations. To reduce problem size of an instance too large to be solved by current quantum hardware, the algorithm relies on correlations. A correlation between a vertex pair quantifies the tendency of the vertices pair being in equal or opposite partitions in an optimum cut. More formally, for a subset $S \subseteq V \times V$ of vertex pairs, correlations are a set $\{b_{uv} \mid uv \in S\}$ where $b_{uv} \in [-1, 1]$. Correlations are called *optimal*, if there is an optimum cut $\delta(W)$ such that $b_{uv} \geq 0$ ($b_{uv} < 0$) if u and v lie in equal (opposite) partitions in $\delta(W)$. In general, the closeness of b_{uv} to 1 (-1) is interpreted as the tendency of u and v lying in equal (opposite) partitions.

In principle, any method to deduce correlations can be used in the algorithm. However, we compute correlations from a solution x^* to the cycle relaxation by

$$b_{uv} := 1 - 2x_{uv}^* \in [-1, 1]. \quad (9)$$

It is well known and can also be seen in our numerical experiments, that cycle relaxation solutions indeed often resemble correlations from an optimum integer solution.

Shrinking. We reduce problem size by identifying vertex pairs which have a large absolute correlation. This process is illustrated in Fig. 2. First, we describe the process of shrinking a single

pair of vertices. To this end, let b_{uv} be a correlation and define

$$\sigma := \begin{cases} \text{sign}(b_{uv}) & b_{uv} \neq 0 \\ 1 & b_{uv} = 0. \end{cases}$$

If $\sigma = 1$ ($\sigma = -1$), we enforce u and v to lie in equal (opposite) partitions. Solving MaxCut on $G = (V, E)$ with this additional constraint is equivalent to solving MaxCut on a graph $G' = (V', E')$, where $V' = V \setminus \{u\}$. For this reduction, edge weights need to be adjusted. For $u \in V$, denote by $\mathcal{N}(u) := \{v \in V \mid uv \in E\}$ the neighborhood of u . For all $t \in \mathcal{N}(u)$, define new weights by

$$w'_{vt} := \begin{cases} \sigma w_{tu} & \text{if } vt \notin E \\ w_{vt} + \sigma w_{tu} & \text{if } vt \in E, \end{cases}$$

compare Fig. 2. All other edge weights remain unchanged. Vertex v now represents a super-vertex containing vertices u and v . Multiple edges are replaced by a single edge. Thus, the reduced MaxCut instance is defined on $G' = (V', E')$ with

$$E' = \left(E \cup \{vt : t \in \mathcal{N}(u)\} \right) \setminus \{ut : t \in \mathcal{N}(u)\},$$

and $V' = V \setminus \{u\}$. Any cut in G' can be translated to a cut in G if σ is known.

This shrinking process is iterated until a target problem-size is reached. We shrink in descending order of the absolute values $|b_{uv}|$. If two vertices to be shrunk have already been identified to the same super-vertex in a previous iteration, the shrinking step is skipped. This avoids possibly contradictory variable fixings. From a different perspective, we only fix variables corresponding to a forest, i.e. a cycle-free subgraph. For the mapping from a solution of the shrunk problem back to a solution of the original instance, it is necessary to keep track of the vertex identifications. In this work, we use QAOA for solving the shrunk problem. However, any suitable method for this task – quantum or classical – can in principle be substituted in our algorithm.

The overall algorithm has three desirable properties which can easily be verified. First, it returns an optimum solution if shrinking with optimal correlations and if the shrunk problem is solved to optimality. Second, if shrinking is performed with non-optimal correlations but the shrunk problem is solved to optimality, the quality of the returned solution will increase when shrinking less vertices. Third, for a fixed shrunk problem, the quality of the returned solution increases with the solution quality of the shrunk problem. Having described the classical algorithmic framework, we now turn to the quantum part.

5 QAOA-Parameter Estimate for Weighted MaxCut

We apply depth-1 QAOA to solve the shrunk MaxCut problem. We restrict our study to depth $p = 1$ for two reasons. First, the high noise level in current quantum hardware prohibits a meaningful execution of large-depth QAOA in practice. This is also the case for the state-of-the-art quantum processor used in our experiments in Section 6. Second, for depth-1 QAOA we are able to derive a high-quality parameter estimate which renders parameter optimization via a classical feedback-loop unnecessary, thus simplifying the execution of QAOA on quantum hardware significantly. However, we emphasize that a successful execution of larger-depth QAOA would lead to improved solutions. Indeed, our experiments in Section 6 reveal that depth-1 QAOA often falls short in returning optimum solutions. Thus, it is desirable to successfully implement large-depth QAOA in the future when quantum hardware improves.

The solution quality returned by QAOA heavily depends on the parameters γ, β . Therefore, deriving good parameters is crucial for its success. The authors of [56] give an analytical expression for the expectation value $F(\gamma, \beta)$ as defined in (6) for depth-1-QAOA applied to unweighted MaxCut. In this section, we extend their results to efficiently derive good parameters for depth-1-QAOA, when applied to weighted MaxCut.

The following statements might serve as a starting point for a further classical parameter optimization. For all instances considered in this work, however, the parameter estimate performs well enough to be used without any further parameter optimization. Next, we state the extended result for weighted MaxCut.

Lemma 5.1. *Let $G = (V, E)$ graph with edge weights $w \in \mathbb{R}^{|E|}$. Let $\gamma, \beta \in \mathbb{R}$ and $F(\gamma, \beta)$ be defined as in (6) with H_C given in (8). Further, for $u, v \in V$, let $\mathcal{N}_u(v)$ be the set of neighbours of v excluding u and denote by $\Lambda(u, v)$ the set of common neighbours of u and v . Then it holds*

$$F(\gamma, \beta) = \sum_{uv \in E} f_{uv}(\gamma, \beta), \quad (10)$$

where

$$f_{uv}(\gamma, \beta) = w_{uv} \left[\frac{1}{2} + \frac{1}{4} \sin(4\beta) \sin(\gamma w_{uv}) \left(\prod_{s \in \mathcal{N}_v(u)} \cos(\gamma w_{us}) + \prod_{t \in \mathcal{N}_u(v)} \cos(\gamma w_{vt}) \right) - \frac{1}{2} \sin^2(2\beta) \sum_{\substack{N \subseteq \Lambda(u, v) \\ |N|=1, 3, 5, \dots}} \prod_{s \in \mathcal{N}_v(u) \setminus N} \cos(\gamma w_{us}) \prod_{t \in \mathcal{N}_u(v) \setminus N} \cos(\gamma w_{vt}) \prod_{r \in N} \sin(\gamma w_{ur}) \sin(\gamma w_{vr}) \right]. \quad (11)$$

Proof. The proof follows the concept from [56] and [64]. We need to evaluate the expectation value of the costs associated to a specific edge $uv \in E$,

$$\begin{aligned} f_{uv} &= \langle + | e^{i\gamma H_C} e^{i\beta H_M} \frac{1}{2} (1 - Z_u Z_v) e^{-i\beta H_M} e^{-i\gamma H_C} | + \rangle \\ &= \frac{1}{2} (1 - \langle + | e^{i\gamma H_C} e^{i\beta H_M} Z_u Z_v e^{-i\beta H_M} e^{-i\gamma H_C} | + \rangle), \end{aligned} \quad (12)$$

where H_C is the MaxCut Hamiltonian defined in (8). For the conjugation with $e^{i\gamma H_C}$, it is convenient to neglect the constant terms. Thus, we define

$$\tilde{H}_C := -\frac{1}{2} Z_u Z_v + \tilde{H}_{C_u} + \tilde{H}_{C_v}$$

with

$$\tilde{H}_{C_u} := -\frac{1}{2} \sum_{s \in \mathcal{N}_v(u)} Z_u Z_s.$$

Now, with $c = \cos 2\beta$ and $s = \sin 2\beta$, it holds

$$e^{i\beta H_M} Z_u Z_v e^{-i\beta H_M} = c^2 Z_u Z_v + s c (Y_u Z_v + Z_u Y_v) + s^2 Y_u Y_v. \quad (13)$$

Each term is conjugated with $e^{i\gamma H_C}$ separately. The key observation is that only terms proportional to products of X -operators will contribute to the expectation value since $\langle + | Y | + \rangle = \langle + | Z | + \rangle = 0$. Thus, the first term in (13) does not contribute. We now turn to the second term. Let $c'_{ij} = \cos(w_{ij}\gamma)$ and $s'_{ij} = \sin(w_{ij}\gamma)$. By using $YZ = -ZY$ we have

$$\begin{aligned} e^{i\gamma H_C} Y_u Z_v e^{-i\gamma H_C} &= e^{i\gamma Z_u Z_v} e^{i2\gamma \tilde{H}_{C_u}} Y_u Z_v \\ &= (Ic'_{uv} - is'_{uv} Z_u Z_v) \prod_{s \in \mathcal{N}_v(u)} (Ic'_{us} - is'_{us} Z_u Z_s) Y_u Z_v. \end{aligned}$$

When expanding the product, there is only a single term that will contribute to the expectation value. This is the term which results from choosing only factors Ic'_{us} in the product. This term is proportional to

$$Z_u Z_v Y_u Z_v = -i X_u.$$

Thus

$$\langle + | e^{i\gamma H_C} Y_u Z_v e^{-i\gamma H_C} | + \rangle = -s'_{uv} \prod_{s \in \mathcal{N}_v(u)} c'_{us}$$

By symmetry, it follows for the third term in (13),

$$\langle + | e^{i\gamma H_C} Z_u Y_v e^{-i\gamma H_C} | + \rangle = -s'_{uv} \prod_{t \in \mathcal{N}_u(v)} c'_{tv}.$$

Now, we turn to the last term in (13). With $YZ = -ZY$, it follows

$$\begin{aligned} e^{i\gamma H_C} Y_u Y_v e^{-i\gamma H_C} &= e^{2i\gamma \tilde{H}_{C_u}} e^{2i\gamma \tilde{H}_{C_v}} Y_u Y_v \\ &= \prod_{s \in \mathcal{N}_v(u)} (c'_{us} I - i s'_{us} Z_u Z_s) \prod_{t \in \mathcal{N}_u(v)} (c'_{tv} I - i s'_{tv} Z_t Z_v) Y_u Y_v. \end{aligned}$$

When expanding the product, only terms proportional to $X_u X_v$ will contribute to the expectation value. If we choose a single term $Z_u Z_s$ in the first product, and a single term $Z_t Z_v$ in the second product such that $s = t$ (i.e. a common neighbor of u and v), the resulting term will be proportional to $X_u X_v$ since

$$Z_u Z_s Z_t Z_v Y_u Y_v = Z_u Z_v Y_u Y_v = -X_u X_v$$

This is also the case for any odd combination of common neighbors. In fact, those are exactly the terms which are proportional to $X_u X_v$. Thus, summation over all odd combinations of common neighbors gives

$$\langle + | e^{i\gamma H_C} Y_u Y_v e^{-i\gamma H_C} | + \rangle = \sum_{\substack{N \subseteq \Lambda(u,v) \\ |N|=1,3,5,\dots}} \prod_{s \in \mathcal{N}_v(u) \setminus N} c'_{us} \prod_{t \in \mathcal{N}_u(v) \setminus N} c_{vt} \prod_{r \in N} s_{ur} s_{vr}.$$

Finally, substituting (13) in (12) yields the result stated in (11). \square

The formula (11) in Lemma 5.1 is cheap to evaluate numerically on sparse instances. For a given edge $uv \in E$, the number of terms in the sum in Eq. (11) is in $O(2^{|\Lambda(u,v)|})$. For sparse instances, $|\Lambda(u,v)|$ is small, often zero, such that the sum in (11) has only few terms. In contrast, the computational cost of the formula derived in [57] and [53] does not depend on $|\Lambda(u,v)|$ but grows linearly with $|N(uv)|$, which is larger than $O(2^{|\Lambda(u,v)|})$ on sparse instances. On the other hand, the number of terms in (11) is very large for dense instances. Then, the formula in [57] and [53] can be evaluated faster.

An often studied class of instances consists of weights that are chosen following a binary distribution in $\{-a, a\}$, $a > 0$. Then, for specific graph topologies, maximizers of $F(\gamma, \beta)$ can be derived analytically from Lemma 5.1, as we show next.

Corollary 5.2. *For triangle-free, d -regular graphs with weights taking values in $\{-a, a\}$, $a > 0$, (10) is maximized for*

$$\gamma = \frac{1}{a} \arctan\left(\frac{1}{\sqrt{d-1}}\right), \quad \beta = \frac{\pi}{8}. \quad (14)$$

Proof. The proof is conducted analogous to [56], Corollary 1, and [64], Corollary 2. Using $\Lambda(u, v) = 0$, $|\mathcal{N}_u(v)| = |\mathcal{N}_v(u)| = d - 1$, $w_{uv} \in \{-a, a\}$, (11) simplifies to

$$\begin{aligned} f_{uv}(\gamma, \beta) &= w_{uv} \left[\frac{1}{2} + \frac{1}{2} \sin(4\beta) \sin(\gamma w_{uv}) \cos^{d-1}(\gamma a) \right] \\ &= \frac{w_{uv}}{2} + \frac{a}{2} \sin(4\beta) \sin(\gamma a) \cos^{d-1}(\gamma a). \end{aligned} \quad (15)$$

By differentiation w.r.t. β and γ , it is easily verified that (14) maximizes (15). Since the maximizers (14) do not depend on uv , they also maximize (10). \square

Although possibly not always being the best choice, Corollary 5.2 motivates the following parameter guess for arbitrary weighted graphs:

$$\bar{\gamma} = \frac{1}{\bar{a}} \arctan \left(\frac{1}{\sqrt{\bar{d}-1}} \right), \quad \bar{\beta} = \frac{\pi}{8}. \quad (16)$$

Here, \bar{a} is the mean of absolute weight values,

$$\bar{a} := \frac{1}{|E|} \sum_{uv \in E} |w_{uv}|,$$

and \bar{d} is the average vertex degree. For triangle-free, regular graphs with weights in $\{-a, a\}$, (16) reduces to (14).

As mentioned above, our numerical experiment show a good performance of parameters (16) such that we use them without further optimization. Of course, better parameters might exist and could possibly be found by a classical parameter optimization. However, this amounts to solving a non-convex, continuous optimization problem which requires multiple estimations of $F(\gamma, \beta)$ via sampling from quantum hardware, thus increasing the runtime of QAOA significantly compared to our approach, which keeps parameters fixed.

Having introduced the algorithmic framework, we are now ready to discuss experimental results from our implementations.

6 Experimental Results

In this section, we present various computational results for the proposed algorithm. All implementations are done in Python. We use the open-source quantum-software development-kit *Qiskit* [70] for quantum circuit construction, ideal quantum simulation as well as quantum hardware communication. For graph operations we use the package *networkx* [71]. Integer models and relaxations are solved via the Python interface of the solver *Gurobi* [72]. Quantum hardware experiments are performed on the quantum backend *ibmq_ehningen* [73] which has 27 superconducting qubits. However, in our experiments we use at most 10 qubits since the influence of noise becomes prohibitively large for higher qubit numbers.

6.1 QAOA Parameter Prediction via (16)

First, we evaluate the performance of the quantum part of our algorithm, which is a depth-1-QAOA with predetermined parameters as stated in (16). As mentioned earlier, the high noise level in the quantum hardware used in our experiments prohibits the use of larger-depth QAOA, which would improve the obtained solutions. Additionally, for depth-1-QAOA we can exploit the parameter estimate (16) which renders parameter optimization unnecessary.

We compare the quality of the estimated parameters to the best possible parameter choice. As a performance metric, we measure the average value of the produced cut size on different weighted MaxCut instances. For each instance, we simulate the quantum algorithm on an ideal, noise-free device, i.e. we numerically evaluate $F(\gamma, \beta)$ via (11). Additionally, we perform experiments on quantum hardware. Here, we evaluate (7) with a sample size of $N = 1024$ and C as defined in (4a). In order to find close-to-optimal parameters, we perform an exhaustive grid search. Parameters (γ, β) are chosen from a grid with step size 0.1 on $[0, \pi/2] \times [0, \pi/2]$. Limiting the parameter search space is eligible because of symmetry relations in QAOA, cf. [74]. In principle, a smaller step size would yield better parameters. In our experiments, however, we observe that a step size of 0.1 is sufficient to capture the characteristics of the parameter-landscape, cf. also Figs. 4 and 7.

We consider three sets of test instances. The first set is constructed solely to investigate the quality of the predetermined parameter choice (16). We construct instances fulfilling all or only some of the assumptions under which these parameters are provably optimal for an ideal quantum device. Recall from Corollary 5.2, that these assumptions are:

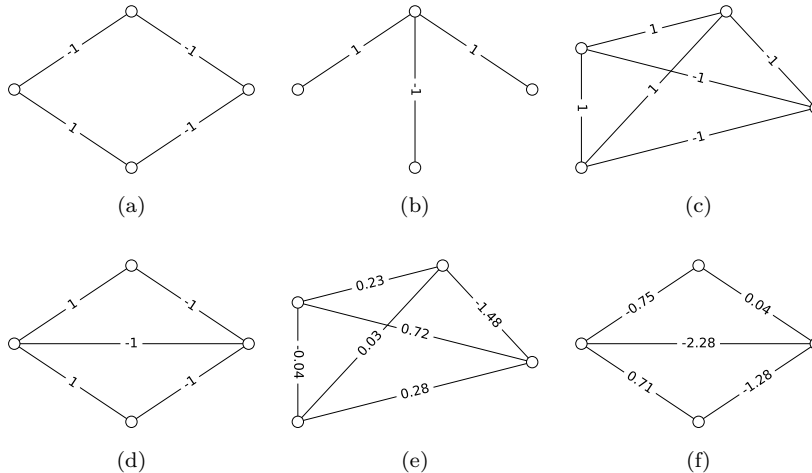


Figure 3: Test instances for the parameter-estimate evaluation.

- (i) The graph is regular.
- (ii) The graph is triangle-free.
- (iii) The weights are chosen from the set $\{-a, a\}$ for some $a > 0$.

Owing to the limitations of quantum hardware, we restrict the size of instances to the minimum which still allows for resembling the desired characteristics. Thus, all instances from the first set have only four vertices and can be solved by hand. They are depicted in Fig. 3. As topologies, we choose a ring, a star, a complete graph and a ring with chord. Weights are drawn either uniformly at random from ± 1 or from a normal distribution. These weight distributions are motivated from spin glass physics cf. e.g. [17].

The second set contains MaxCut instances which result from shrinking a 2×3 grid with ± 1 weights: an instance considered in the next section, where we evaluate the combination of shrinking and QAOA. Instance names of the second set are of the form “2x3gns”. Here, n denotes the number of vertices in the shrunk graph and s marks whether the cycle relaxation was used for shrinking (“c”) or random edges were shrunk (“r”), see Section 6.2 for details. If random shrinking and cycle-relaxation-shrinking led to the same instance, “rc” is used.

The third set is constructed to investigate the scalability of our parameter estimate. Here, we consider a 10-regular graph on 100 vertices (“100reg”) as well as a 100-vertex ring with 20 additional edges inserted such that the graph remains triangle-free (“100trf”). These two instances have normal distributed weights. Moreover, we consider four 100-vertex Erdős–Rényi random graph ensembles with densities $d \in \{0.05, 0.1, 0.15, 0.2\}$ (“100randd”). These graphs are unweighted, i.e., edges have unit weights. It is known that random unweighted MaxCut undergoes a phase transition at the critical edge density of $d^* = 1/|V|$, cf. [75]. If $d < d^*$, the expected number of edges not in an optimum cut is $\Theta(1)$ for large $|V|$. If $d > d^*$, the expected number of edges not in an optimum cut jumps to $\Theta(|V|)$. Thus, we consider four Erdős–Rényi ensembles: a sub-critical ensemble with $d = 0.05$, a critical ensemble with $d = d^* = 0.1$ and two super-critical ensembles with $d \in \{0.15, 0.2\}$. Here, we average over 20 graphs from each ensemble.

Table 1 summarizes the experimental results. Instance names of the first set correspond to sub-figures in Fig. 3. For each instance, we mark which of assumptions (i)-(iii) are met. Furthermore, we measure the relative deviation of $F(\bar{\gamma}, \bar{\beta})$ from the maximum of $F(\gamma, \beta)$,

$$\frac{\max F(\gamma, \beta) - F(\bar{\gamma}, \bar{\beta})}{\max F(\gamma, \beta) - \min F(\gamma, \beta)} \in [0, 1].$$

Thus, a value of 0 means that indeed the maximum is hit, whereas 1 means that we hit the minimum instead. Here, we estimate the true maxima and minima via the respective values from the grid search. Analogously, for the real quantum experiment, we measure

$$\frac{\max\langle C\rangle(\gamma, \beta) - \langle C\rangle(\bar{\gamma}, \bar{\beta})}{\max\langle C\rangle(\gamma, \beta) - \min\langle C\rangle(\gamma, \beta)} \in [0, 1] .$$

As expected, the deviation of $F(\bar{\gamma}, \bar{\beta})$ from the optimum value of $F(\gamma, \beta)$ increases when the instance violates more assumptions from (i)-(iii). The maximum observed deviation is 10% on instance f which violates all assumptions. From an integer-programming point of view, 10% might seem a large deviation. However, we stress that we do not compare single solution values but expectation values as QAOA is a probabilistic algorithm. Of course, the best solution in a reasonably sized sample will be better than the expectation value.

In Table 1, the values of $\langle C\rangle(\bar{\gamma}, \bar{\beta})$, measured with the real quantum backend, roughly follow the qualitative behavior of $F(\bar{\gamma}, \bar{\beta})$ across all instances. Quantitatively, the values from real hardware always lie slightly above the corresponding values from the ideal simulation. This means, that our parameter estimate performs slightly worse on real hardware than in theory. Of course, in real quantum hardware, many physical effects influence the outcome of QAOA which are all not considered in the derivation of (16). With this in mind, it is even more encouraging that our parameter estimate hits the optimum within a maximum observed deviation of at most 13%.

Considering the instances “2x3gns”, resulting from shrinking the 2×3 grid, observed deviations are typically less than for the artificial instances a - f. This further motivates the use of QAOA with parameters (16), when combined with shrinking as investigated in the next section.

The large instances with 100 vertices could not be executed on real hardware (“-” in Table 1). Still, we can evaluate (11) numerically. We observe a good performance of the parameter estimate in the numerical simulations for all large instances with a maximum deviation of 1 %. Although the estimate seems to become slightly worse with increasing density, these results indicate a high scalability of the proposed method.

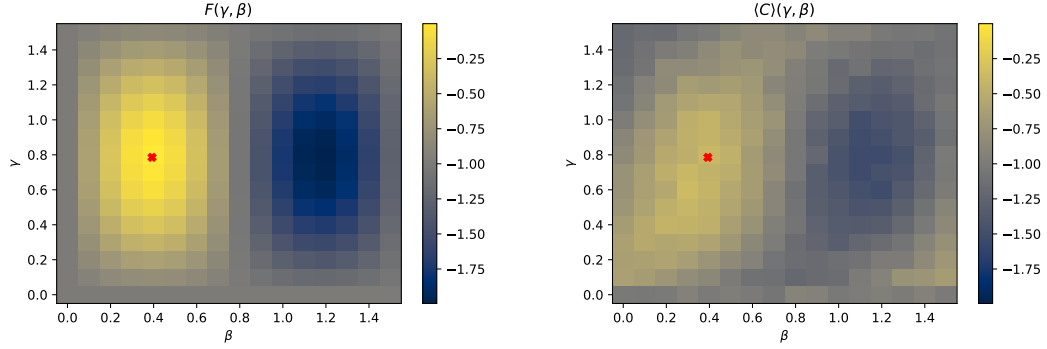
To further illustrate the differences between ideal simulation and real experiment, $F(\gamma, \beta)$ and $\langle C\rangle(\gamma, \beta)$ are visualized in Fig. 4. Although not being exactly identical, the data from the experiment qualitatively follows the simulation. It is worth noting, that the absolute values in the experiment are usually smaller than in the simulation. The observed differences between simulation and experiment are due to noise effects in quantum hardware. Analogue figures for other instances appear in Appendix A.1.

Summarizing, our results show that the parameter estimate (16) performs well, even on instances that do not satisfy the assumptions where it is provably optimal. These results encourage us to use of QAOA without further parameter optimization in the upcoming section where we combine shrinking with QAOA to solve MaxCut instances too large to be handled by quantum hardware alone.

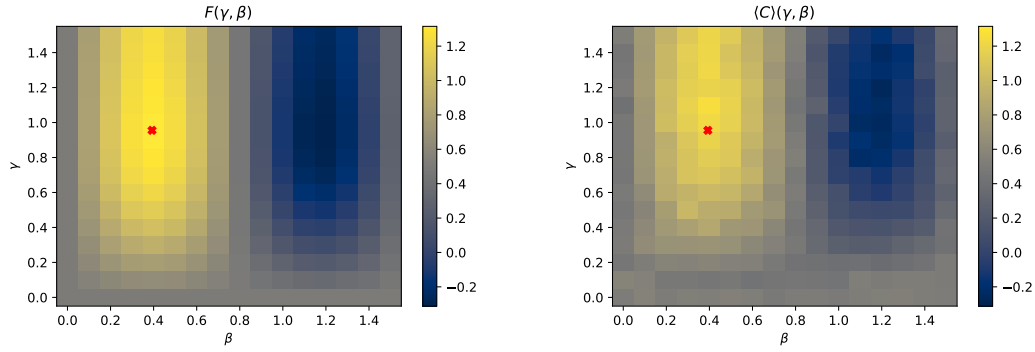
6.2 Combining Shrinking with QAOA

In this section, we combine shrinking via the cycle relaxation, as described in Section 4, with QAOA. Again, instance sizes are kept small due to limitations of quantum hardware. As in the previous section, graph topologies and weight distributions are motivated by spin glass physics. We emphasize that all instances can be solved by classical integer programming quickly. Thus, the experiments in this section should be considered as a proof-of-principle rather than a performance-benchmark.

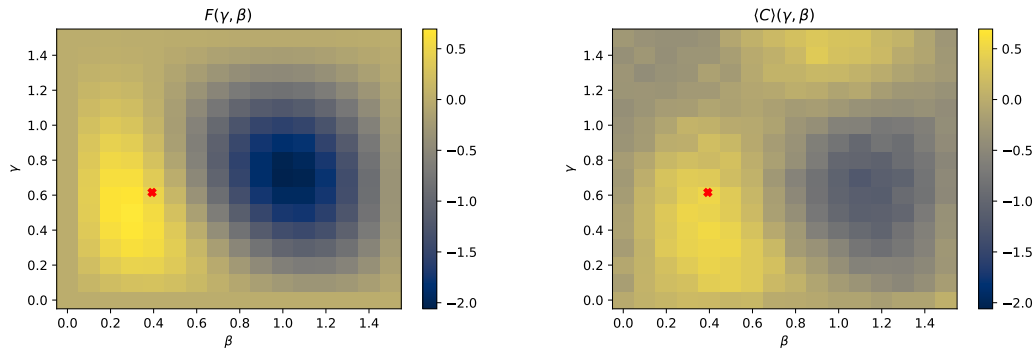
When computing the cycle relaxation on sparse graphs, we model a complete graph and assign zero weights to edges not present in the sparse graph. Thus, all odd-cycle inequalities belong to triangles and are of the form (2a)-(2d). We remark, that this relaxation has the same objective value as the sparse odd-cycle relaxation (1a)-(1c) since the polyhedron defined by (1b)-(1c) is a projection of the polyhedron (2a)-(2d) along a direction orthogonal to the cost vector in (1a). We work with the dense cycle-relaxation for two reasons. First, the dense formulation has variables for all vertex pairs, not only for edges present in the sparse graph. This allows to shrink vertex



(a) Instance a.



(b) Instance b.



(c) Instance c.

Figure 4: Visualized results for QAOA parameter-estimate on instances a, b and c from Fig. 3. The x- and y-axis represent values of the parameters β and γ , respectively. The red cross marks the estimate in (16). The color encodes the expectation value (left) or the average (right) of the cut size. On the left, we mimic an ideal quantum device by evaluation of (11). On the right, values are results from the quantum hardware. Here, every pixel represents the average taken over 1,024 samples.

Instance	Regular	Triangle-free	$w_{ij} \in \{-a, a\}$	$\frac{\max F(\gamma, \beta) - F(\bar{\gamma}, \bar{\beta})}{\max F(\gamma, \beta) - \min F(\gamma, \beta)}$	$\frac{\max \langle C \rangle(\gamma, \beta) - \langle C \rangle(\bar{\gamma}, \bar{\beta})}{\max \langle C \rangle(\gamma, \beta) - \min \langle C \rangle(\gamma, \beta)}$
a	✓	✓	✓	0.0	0.03
b	✗	✓	✓	0.0	0.02
c	✓	✗	✓	0.07	0.02
d	✗	✗	✓	0.05	0.09
e	✓	✗	✗	0.08	0.08
f	✗	✗	✗	0.10	0.13
2x3g2r	✓	✓	✓	0.0	0.0
2x3g3rc	✓	✗	✓	0.06	0.06
2x3g4c	✓	✓	✗	0.0	0.0
2x3g4r	✗	✓	✓	0.0	0.01
2x3g5c	✗	✗	✗	0.0	0.04
2x3g5c	✗	✗	✓	0.0	0.05
2x3g6rc	✗	✗	✓	0.0	0.0
100reg	✓	✗	✗	0.007	-
100trf	✗	✓	✗	0.02	-
100rand0.05	✗	✗	✓	0.0	-
100rand0.1	✗	✗	✓	0.0	-
100rand0.15	✗	✗	✓	0.007	-
100rand0.2	✗	✗	✓	0.01	-

Table 1: Experimental results for evaluating the QAOA-parameter-estimate. In column “Instance”, a - f refer to Fig. 3. In columns “Regular”, “Triangle-free” and “ $w_{ij} \in \{-a, a\}$ ” fulfilled assumptions of Cor. 5.2 are marked. The second last column gives the relative deviation of $F(\bar{\gamma}, \bar{\beta})$ from the optimal value. The values are calculated by (11). The last column gives the deviation of $\langle C \rangle(\bar{\gamma}, \bar{\beta})$ from the optimum. Here, real quantum hardware was used.

pairs not connected by an edge in the sparse graph, i.e. vertex pairs corresponding to an edge with zero weight in the dense model. Second, this formulation can be implemented straightforwardly by simply enumerating all triangles. Of course, this implementation is not efficient compared to state-of-the-art separation methods. However, since we aim at a proof-of-concept and considered instances are small, this approach is sufficient for our numerical experiments.

Table 2 summarizes the instance data and results. Concerning the runtime for the small instances with up to 16 vertices, solving the cycle relaxation took far less than one second while the total quantum runtime for 10,000 executions of QAOA was roughly 2 seconds. We also considered two larger instances from literature, available in [76]. The first is “t2g10_5555”, a 10×10 toroidal grid with 100 vertices and normal distributed weights. The second is “ising2.5-100_5555”, the fully connected graph K_{100} on 100 vertices with weights decaying exponentially with distance. Both instances are an order of magnitude larger than the capabilities of current digital QC hardware. However, they can still be handled by classical branch-and-cut based on cycle relaxations.³ For both large instances, solving the cycle relaxation took less than one minute, while the runtime for solving the shrunk instance on the quantum machine was roughly 5 seconds.

In Table 2, we compare the achieved approximation ratio using the real quantum computer without shrinking, $r_{|V|}$, to the approximation ratio when shrinking to four vertices, r_4 . In this work, we define the approximation ratio as

$$r := \frac{\langle C \rangle - C_{\min}}{C_{\max} - C_{\min}} \in [0, 1], \quad (17)$$

where $\langle C \rangle$ is the average size of a returned cut, C_{\min} and C_{\max} are the minimum and maximum cut sizes, respectively. For all of the small instances, we observe that shrinking significantly increases

³Although the instance “ising2.5-100_5555” is fully connected, the cycle relaxation is still strong due to the specific structured weight distribution which suppresses weights of distant vertices.

Instance	Graph	$ V $	$ E $	Weights	r_0	r_1	$r_{\lfloor V /2 \rfloor}$	$r_{ V -6}$	$r_{ V -4}$	$r_{ V -2}$
2x3b	2×3 grid	6	7	± 1	53 %	66 %	98 %	53 %	90 %	100 %
k6b	K_6	6	15	± 1	47 %	68 %	86 %	47 %	73 %	94 %
k6n	K_6	6	15	\mathcal{N}	44 %	38 %	79 %	44 %	56 %	94 %
3x3b	3×3 grid	9	12	± 1	57 %	71 %	90 %	83 %	90 %	96 %
k10b	K_{10}	10	45	± 1	69 %	71 %	82 %	76 %	74 %	88 %
k10n	K_{10}	10	45	\mathcal{N}	51 %	55 %	79 %	73 %	74 %	98 %
4x4b	4×4 grid	16	24	± 1	-	-	73 %	80 %	86 %	98 %
t2g10_5555	10×10 torus grid	100	200	\mathcal{N}	-	-	-	96 %	98 %	99 %
ising2.5-100_5555	K_{100}	100	4950	\mathcal{N} , decaying	-	-	-	98 %	99 %	99 %

Table 2: Instance data and results for evaluating the shrinking algorithm. $|V|$ and $|E|$ are the number of vertices and edges, respectively. In column “Weights”, ± 1 abbreviates the uniform distribution on $\{-1, 1\}$, \mathcal{N} abbreviates the standard normal distribution and “ \mathcal{N} , decaying” is a normal distribution decaying proportional to euclidean distance. In columns r_k , we state the achieved approximation ratio when shrinking k vertices and solving the shrunk problem by depth-1-QAOA on actual quantum hardware. A “-” indicates that the problem instance is too large for the quantum hardware used in our experiments.

the approximation ratio. For the larger instances with 16 and 100 vertices, running QAOA was not possible without shrinking below 11 vertices due to hardware limitations (“-” in Table 2). Notably, for the first instance, shrinking only two vertices yields an increase in approximation ratio of almost 40 %.

Fig. 5 allows a more detailed analysis of the algorithm for the first two instances from Table 2. Here, we run the algorithm with different settings. First, we alter the number of shrunk vertices (x-axis in Fig. 5). In general, the potential, i.e. the best possible cut value, will degrade when shrinking more vertices since there might not exist an optimum solution with the imposed correlations. This is the case if and only if the imposed correlations are not optimal. In this case, even when the shrunk problem is solved to optimality, the recreated solution cannot be optimal. On the other hand, shrinking more vertices reduces the problem size, which might lead to better solutions for the shrunk problem, especially when using near-future quantum hardware. The second setting we vary are the procedures for computing correlations (corresponding to different colors in Fig. 5). This allows to investigate the influence of the correlation quality on the overall performance. Two methods are used:

1. Correlations inferred from the cycle relaxation, defined in (9) (blue lines in Fig. 5).
2. All correlations are zero which results in shrinking random vertex pairs with $\sigma = 1$ (red lines in Fig. 5).

Lastly, we apply different solution methods (corresponding to different line marks in Fig. 5) for the shrunk problem in order to investigate the influence of the sub-problem solution quality on the overall performance. The sub-problem is solved in four different ways:

1. We solve the shrunk problem to optimality by integer programming (solid lines). This yields an upper bound on the performance of our algorithm.
2. We solve the shrunk problem by a depth-1-QAOA with parameters predetermined by (16), executed 10,000 times on an ideal quantum simulator (dashed-dotted lines).
3. We solve the problem exactly as in 2, but with real quantum hardware instead of an ideal quantum simulator (dashed lines).
4. We solve the shrunk problem randomly by flipping a coin for each vertex, i.e. we assign each vertex to either partition with probability $1/2$ (dotted lines). When noise in the real quantum

machine becomes large (called *decoherence*), the quantum computer effectively performs the coin-flipping heuristic.

Considering the approximation ratio when solving the shrunk problem to optimality (solid lines), we note that shrinking with correlations from the cycle relaxation (blue) always returns optimal solutions. This means that the inferred correlations (9) are indeed optimal. Thus, if sub-optimal solutions to the original problem are retrieved when running QAOA instead of an exact algorithm for the shrunk problem, the degrade in solution quality must be attributed purely to QAOA. As expected, the potential decreases when shrinking randomly (red solid lines). Here, correlations are sub-optimal which means that an optimal solution with the imposed correlations does not exist.

Now, we turn to the approximation ratio when solving the shrunk problem on the ideal quantum simulator (dashed-dotted lines). As expected, when shrinking with optimal correlations inferred from the cycle relaxation (blue), the approximation ratio monotonically increases with vertex deletions. A smaller sub-problem can be better approximated by the quantum algorithm. Rather interestingly, an increase in approximation ratio when deleting more vertices can sometimes be observed even when shrinking randomly (red). Here, the better approximability of the sub-problem by the quantum algorithm over-compensates the degrade in potential caused by shrinking sub-optimally. These results highlight the strong limitation of QAOA at depth $p = 1$. Indeed, other studies suggest that $p \gtrsim 11$ is required for QAOA to outperform classical algorithms, which is intractable for current quantum hardware platforms [13, 54].

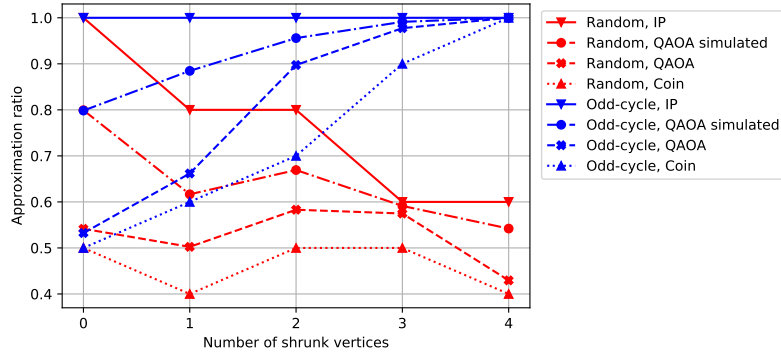
Presumably, the most interesting case is when the shrunk problem is solved on the real quantum machine (dashed lines). The approximation ratio qualitatively follows the ideal simulation for both, optimal correlations (blue) and random shrinking (red). However, as expected, the quantum hardware always performs worse than the ideal simulation. Of course, this is due to noise effects in real hardware. Notably, we observe a maximum approximation-ratio at 2 deleted vertices in both instances when shrinking randomly (red). Here, the trade-off between potential degrade due to sub-optimal shrinking and performance gain due to increased approximability is optimal. Finally, we note a significant advantage of QAOA over the coin-flipping-heuristic (dotted lines), when shrinking one or more vertices. Without shrinking, i.e. zero shrunk vertices, we observe that noise effects take over, and QAOA effectively flips a coin for every vertex.

Corresponding figures for instances k6n and 3x3b appear in Appendix A.2. The two key observations are the same as in Fig. 5: First, the cycle relaxation yields optimal correlations. Second, maxima in the approximation ratio for QAOA on real hardware are present when shrinking randomly. We do not provide figures for the remaining instances from Table 2 because conclusions are similar to the previously discussed instances.

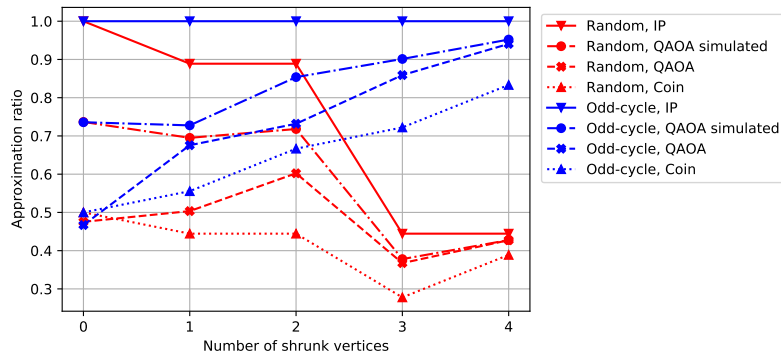
Summarizing, the results indicate that the proposed shrinking method can indeed reduce problem size significantly without degrading solution quality: In our experiments, shrinking with the cycle relaxation always preserved optimality, i.e. inferred correlations are optimal. This is beneficial for quantum computation on noisy hardware of limited size. When shrinking optimally, the performance of QAOA always increased with the number of deleted vertices. From this, we conclude that QAOA at depth $p = 1$ is strongly limited in finding high-quality solutions, even for small instances. Interestingly, when shrinking sub-optimally, we observed an optimal trade-off between potential-loss and increased approximability of the reduced problem. By combining linear programming with QAOA, we were able to solve MaxCut instances from literature an order of magnitude larger than the capabilities of current digital quantum hardware. Although our experiments yield only a proof-of-principle, they encourage the combination of quantum algorithms with classical branch-and-cut, when QC approaches regimes where it outperforms classical heuristics.

6.3 Comparison of LP Shrinking to RQAOA and Goemans-Williamson

As mentioned earlier, any method for obtaining variable correlations can be substituted in the shrinking procedure from Section 4 by substituting Equation (9) appropriately. In particular, using correlations obtained by QAOA and recalculating these correlations after every shrinking step, recovers the well-known RQAOA [53]. In this section, we compare the quality of LP-based



(a) Instance 2x3b.



(b) Instance k6b.

Figure 5: Results for evaluating the shrinking-algorithm with different setting. Shown is the approximation ratio, defined in (17), versus the number of shrunk vertices. In the legend, “Random” stands for random shrinking while “Odd-cycle” stands for correlations given by (9). “IP”, “QAOA simulated”, “QAOA” and “Coin” refer to different sub-problem solution methods as discussed in the main text body.

shrinking procedure to RQAOA. To this end, we shrink random MaxCut instances via both, RQAOA and the LP-based method proposed in this work.

For a fair comparison, we recalculate the cycle relaxation after every shrinking step, analogous to RQAOA, which continuously updates QAOA correlations. QAOA correlations are obtained by evaluating (11) at parameters estimated by (16). Although estimated parameters can be sub-optimal in principle, the results in Sec. 6.1 reveal a good performance of the estimated parameters on random MaxCut instances, cf. Table 1.

As instances, we choose the same Erdős–Rényi graphs as in Sec. 6.1. That is, we consider graphs on 100 nodes with edge densities $d \in \{0.05, 0.1, 0.15, 0.2\}$. Again, the motivation is to cover densities below and above the critical density of $d^* = 0.1$. Considering runtimes, solving a single LP relaxation takes ~ 60 s while calculating RQAOA correlations is in the order of 1 s.

In Fig. 6 we visualize the results. Analogous to the previous section, we plot the number of shrunk vertices versus the average approximation ratio when solving the shrunk problem to optimality. This allows us to compare the LP-based shrinking algorithm to RQAOA. First, when considering low density instances with $d = 0.05$ (blue lines in Fig. 6), we observe that LP-shrinking (dots) yields higher average approximation ratios than RQAOA (crosses) for all numbers of shrunk vertices. LP shrinking constantly yields approximation ratios above 99.7 % whereas the RQAOA approximation ratio decreases with increasing number of shrunk vertices below 96.5 %. For the critical density $d = 0.1$ (orange) LP performs slightly worse than for $d = 0.05$, while at the same time, RQAOA performs slightly better, thus reducing the advantage of LP. However, LP still outperforms RQAOA for all numbers of shrunk vertices. For the high density instances with $d = 0.15$ (green), the performance of LP decreases further, in particular when shrinking more than half of the vertices. At the same time, the performance of RQAOA increases compared to density $d = 0.1$. However, LP still outperforms RQAOA except when shrinking more than 70 vertices. This trend continues. For higher densities, the approximation ratio of LP shrinking decreases more rapidly with the number of shrunk vertices. At the same time, RQAOA achieves larger approximation ratios for higher densities. Still, at a density of $d = 0.2$ (red), LP outperforms RQAOA up to shrinking 50 vertices. Our results are in agreement with previous studies, which revealed that the cycle relaxation is strong on sparse instances [31, 30, 36, 18].

For completeness, we also compare RQAOA and LP-based shrinking to the well-known classical Goemans-Williamson algorithm, which uses positive semidefinite optimization. To this end, we perform the randomized rounding algorithm for every instance and calculate the average approximation ratio for each ensemble (solid lines). Both, LP-shrinking and RQAOA outperform the Goemans-Williamson algorithm for almost all densities and numbers of shrunk vertices. The only exceptions are the high-density instances with $d = 0.2$ (red) where Goemans-Williamson outperforms LP when shrinking more than 60 vertices.

In summary, we observe that linear programming yields high-quality correlations for instances with densities of up to 20 %, which covers a very wide range of problem classes. Even on denser instances, RQAOA outperforms LP only when shrinking more than half of the vertices. Similar to Section 6.2, we conclude that depth-1-QAOA often produces sub-optimal correlations and larger QAOA depths are required to outperform classically obtained correlations. However, larger QAOA depths complicates parameter optimization, potentially remedying the runtime advantage over classical methods.

7 Conclusion and Outlook

In this work, we proposed a hybrid quantum-classical heuristic algorithm for the maximum cut problem. The guiding idea is to combine the ability of classical integer programming to solve large relaxations with the promise of quantum optimization to find high-quality solutions quickly. The algorithm is particularly well-suited for integration in classical integer programming for two reasons: First, it relies on relaxation solutions and, second, it helps to avoid enumeration in classical branch-and-cut. More specifically, we use the well-known technique of graph shrinking to reduce problem size such that it can be handled by quantum hardware with limited resources. To this end, we shrink according to an optimum of the cycle relaxation of the cut polytope. Furthermore, we

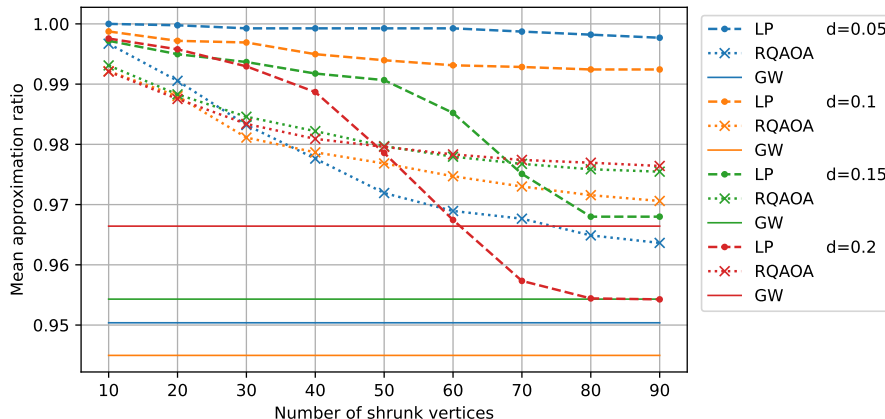


Figure 6: Comparison of LP-based shrinking to RQAOA and Goemans-Williamson. We plot the number of shrunk vertices versus the average approximation ratio. Instances are Erdős-Rényi random graphs on 100 vertices with different densities $d \in \{0.05, 0.1, 0.15, 0.2\}$. Data points are averaged over 20 instances. For completeness, we also include the average approximation ratio for the Goemans-Williamson rounding algorithm (solid lines).

improved the applicability of depth-1 QAOA for weighted MaxCut, which builds the quantum part in the hybrid algorithm, by deriving optimal parameters for instances on regular and triangle-free graphs with weights following a binary distribution. This result motivates a parameter estimate for arbitrary instances.

Our experiments give a proof-of-principle for the applicability of the proposed methods. Although all considered instances can be solved in reasonable time by purely classical algorithms, the results indicate a potential benefit for integer programming, when QC improves. First, the proposed QAOA parameter estimate works well in practice. This improves the applicability of depth-1 QAOA since it renders classical parameter optimization unnecessary. Second, when combining shrinking with QAOA, we observed that linear programming can shrink problem size significantly without losing optimality. In particular, linear programming outperforms depth-1 RQAOA on sparse instances. Furthermore, we observed that shrinking is indeed beneficial for QAOA when executed on current quantum hardware. Our results indicate that depth-1 QAOA is strongly limited in finding optimum solutions and quantum algorithms of higher quality are needed for practical utility. Of course, a more thorough evaluation on a wider range of instances is needed to investigate the performance of our method in more detail.

A direction of future research is the incorporation of characteristics of quantum algorithms and quantum hardware in the process of shrinking. It is known, that QAOA performs worse on certain types of graphs, e.g. bipartite graphs. From a hardware perspective, sparse graphs simplify the implementation of QAOA. In the process of shrinking, one can try to avoid or produce such specific graph characteristics. Moreover, other techniques for deriving (optimal) correlations exist in literature. Their performance in our framework needs to be further studied. Extending the set of test instances allows deeper insights into the instance-dependence of the proposed algorithm. Another field of ongoing research is the quantum part which may be replaced by higher-depth QAOA or variants like warm-start QAOA or even by different algorithmic paradigms like quantum annealing.

References

- [1] E. Robert Bixby, Mary Fenelon, Zonghao Gu, Ed Rothberg, and Roland Wunderling. Mip: Theory and practice — closing the gap. In M. J. D. Powell and S. Scholtes, editors, *System Modelling and Optimization*, pages 19–49, Boston, MA, 2000. Springer US.

- [2] Robert E. Bixby. Solving real-world linear programs: A decade and more of progress. *Operations Research*, 50(1):3–15, 2002. [arXiv:https://doi.org/10.1287/opre.50.1.3.17780](https://doi.org/10.1287/opre.50.1.3.17780), [doi:10.1287/opre.50.1.3.17780](https://doi.org/10.1287/opre.50.1.3.17780).
- [3] Thorsten Koch, Timo Berthold, Jaap Pedersen, and Charlie Vanaret. Progress in mathematical programming solvers from 2001 to 2020. *EURO Journal on Computational Optimization*, 10:100031, 2022. [doi:10.1016/j.ejco.2022.100031](https://doi.org/10.1016/j.ejco.2022.100031).
- [4] Ambros Gleixner, Gregor Hendel, Gerald Gamrath, Tobias Achterberg, Michael Bastubbe, Timo Berthold, Philipp M. Christophel, Kati Jarck, Thorsten Koch, Jeff Linderoth, Marco Lübbecke, Hans D. Mittelmann, Derya Ozyurt, Ted K. Ralphs, Domenico Salvagnin, and Yuji Shinano. MIPLIB 2017: Data-Driven Compilation of the 6th Mixed-Integer Programming Library. *Mathematical Programming Computation*, 2021. [doi:10.1007/s12532-020-00194-3](https://doi.org/10.1007/s12532-020-00194-3).
- [5] Nikolaž Moll, Panagiotis Barkoutsos, Lev S. Bishop, Jerry M. Chow, Andrew Cross, Daniel J. Egger, Stefan Filipp, Andreas Fuhrer, Jay M. Gambetta, Marc Ganzhorn, Abhinav Kandala, Antonio Mezzacapo, Peter Müller, Walter Riess, Gian Salis, John Smolin, Ivano Tavernelli, and Kristan Temme. Quantum optimization using variational algorithms on near-term quantum devices. *Quantum Science and Technology*, 3(3):030503, jun 2018. [doi:10.1088/2058-9565/aab822](https://doi.org/10.1088/2058-9565/aab822).
- [6] Amira Abbas, Andris Ambainis, Brandon Augustino, Andreas Bärtzchi, Harry Buhrman, Carleton Coffrin, Giorgio Cortiana, Vedran Dunjko, Daniel J. Egger, Bruce G. Elmegreen, Nicola Franco, Filippo Fratini, Bryce Fuller, Julien Gacon, Constantin Gonciulea, Sander Gribling, Swati Gupta, Stuart Hadfield, Raoul Heese, Gerhard Kircher, Thomas Kleinert, Thorsten Koch, Georgios Korpas, Steve Lenk, Jakub Marecek, Vanio Markov, Guglielmo Mazzola, Stefano Mensa, Naeimeh Mohseni, Giacomo Nannicini, Corey O’Meara, Elena Peña Tapia, Sebastian Pokutta, Manuel Proissl, Patrick Rebentrost, Emre Sahin, Benjamin C. B. Symons, Sabine Törnøw, Victor Valls, Stefan Woerner, Mira L. Wolf-Bauwens, Jon Yard, Sheir Yarkoni, Dirk Zechiel, Sergiy Zhuk, and Christa Zoufal. Quantum optimization: Potential, challenges, and the path forward, 2023. [arXiv:2312.02279](https://arxiv.org/abs/2312.02279).
- [7] Tameem Albash and Daniel A. Lidar. Demonstration of a scaling advantage for a quantum annealer over simulated annealing. *Phys. Rev. X*, 8:031016, Jul 2018. [doi:10.1103/PhysRevX.8.031016](https://doi.org/10.1103/PhysRevX.8.031016).
- [8] Catherine C. McGeoch and Pau Farré. Milestones on the quantum utility highway: Quantum annealing case study. *ACM Transactions on Quantum Computing*, 5(1), dec 2023. [doi:10.1145/3625307](https://doi.org/10.1145/3625307).
- [9] Edward Farhi, Jeffrey Goldstone, and Sam Gutmann. A quantum approximate optimization algorithm, 2014. [arXiv:1411.4028](https://arxiv.org/abs/1411.4028).
- [10] Matthew P. Harrigan, Kevin J. Sung, Matthew Neeley, Kevin J. Satzinger, Frank Arute, Kunal Arya, Juan Atalaya, Joseph C. Bardin, Rami Barends, Sergio Boixo, Michael Broughton, Bob B. Buckley, David A. Buell, Brian Burkett, Nicholas Bushnell, Yu Chen, Zijun Chen, Ben Chiaro, Roberto Collins, William Courtney, Sean Demura, Andrew Dunsworth, Daniel Eppens, Austin Fowler, Brooks Foxen, Craig Gidney, Marissa Giustina, Rob Graff, Steve Habegger, Alan Ho, Sabrina Hong, Trent Huang, L. B. Ioffe, Sergei V. Isakov, Evan Jeffrey, Zhang Jiang, Cody Jones, Dvir Kafri, Kostyantyn Kechedzhi, Julian Kelly, Seon Kim, Paul V. Klimov, Alexander N. Korotkov, Fedor Kostritsa, David Landhuis, Pavel Laptev, Mike Lindmark, Martin Leib, Orion Martin, John M. Martinis, Jarrod R. McClean, Matt McEwen, Anthony Megrant, Xiao Mi, Masoud Mohseni, Wojciech Mroczkiewicz, Josh Mutus, Ofer Naaman, Charles Neill, Florian Neukart, Murphy Yuezhen Niu, Thomas E. O’Brien, Bryan O’Gorman, Eric Ostby, Andre Petukhov, Harald Putterman, Chris Quintana, Pedram Roushan, Nicholas C. Rubin, Daniel Sank, Andrea Skolik, Vadim Smelyanskiy, Doug Strain, Michael Streif, Marco Szalay, Amit Vainsencher, Theodore White, Z. Jamie Yao, Ping Yeh, Adam Zalcman,

- Leo Zhou, Hartmut Neven, Dave Bacon, Erik Lucero, Edward Farhi, and Ryan Babbush. Quantum approximate optimization of non-planar graph problems on a planar superconducting processor. *Nature Physics*, 17(3):332–336, feb 2021. doi:[10.1038/s41567-020-01105-y](https://doi.org/10.1038/s41567-020-01105-y).
- [11] G. G. Guerreschi and A. Y. Matsuura. Qaoa for max-cut requires hundreds of qubits for quantum speed-up. *Scientific Reports*, 9(1), May 2019. doi:[10.1038/s41598-019-43176-9](https://doi.org/10.1038/s41598-019-43176-9).
- [12] Michael Jünger, Elisabeth Lobe, Petra Mutzel, Gerhard Reinelt, Franz Rendl, Giovanni Rinaldi, and Tobias Stollenwerk. Quantum annealing versus digital computing: An experimental comparison. *ACM J. Exp. Algorithmics*, 26, jul 2021. doi:[10.1145/3459606](https://doi.org/10.1145/3459606).
- [13] Danylo Lykov, Jonathan Wurtz, Cody Poole, Mark Saffman, Tom Noel, and Yuri Alexeev. Sampling frequency thresholds for quantum advantage of quantum approximate optimization algorithm, 2022. arXiv:[2206.03579](https://arxiv.org/abs/2206.03579).
- [14] Matteo Fischetti and Andrea Lodi. *Heuristics in Mixed Integer Programming*. John Wiley & Sons, Ltd, 2011. doi:[10.1002/9780470400531.eorms0376](https://doi.org/10.1002/9780470400531.eorms0376).
- [15] Tobias Achterberg, Timo Berthold, and Gregor Hendel. Rounding and propagation heuristics for mixed integer programming. In Diethard Klatte, Hans-Jakob Lüthi, and Karl Schmedders, editors, *Operations Research Proceedings 2011*, pages 71–76, Berlin, Heidelberg, 2012. Springer Berlin Heidelberg.
- [16] Francisco Barahona, Martin Grötschel, Michael Jünger, and Gerhard Reinelt. An application of combinatorial optimization to statistical physics and circuit layout design. *Operations Research*, 36(3):493–513, 1988.
- [17] Frauke Liers, Michael Jünger, Gerhard Reinelt, and Giovanni Rinaldi. *Computing Exact Ground States of Hard Ising Spin Glass Problems by Branch-and-Cut*, chapter 4, pages 47–69. John Wiley & Sons, Ltd, 2004. arXiv:<https://onlinelibrary.wiley.com/doi/pdf/10.1002/3527603794.ch4>, doi:[10.1002/3527603794.ch4](https://doi.org/10.1002/3527603794.ch4).
- [18] Thorsten Bonato, Michael Jünger, Gerhard Reinelt, and Giovanni Rinaldi. Lifting and separation procedures for the cut polytope. *Mathematical Programming*, 146(1):351–378, Aug 2014. doi:[10.1007/s10107-013-0688-2](https://doi.org/10.1007/s10107-013-0688-2).
- [19] Richard M. Karp. Reducibility among combinatorial problems. In Raymond E. Miller, James W. Thatcher, and Jean D. Bohlinger, editors, *Complexity of Computer Computations: Proceedings of a symposium on the Complexity of Computer Computations, held March 20–22, 1972, at the IBM Thomas J. Watson Research Center, Yorktown Heights, New York, and sponsored by the Office of Naval Research, Mathematics Program, IBM World Trade Corporation, and the IBM Research Mathematical Sciences Department*, pages 85–103, Boston, MA, 1972. Springer US. doi:[10.1007/978-1-4684-2001-2_9](https://doi.org/10.1007/978-1-4684-2001-2_9).
- [20] F. Hadlock. Finding a maximum cut of a planar graph in polynomial time. *SIAM Journal on Computing*, 4(3):221–225, 1975. arXiv:<https://doi.org/10.1137/0204019>, doi:[10.1137/0204019](https://doi.org/10.1137/0204019).
- [21] Frauke Liers and G. Pardella. Partitioning planar graphs: A fast combinatorial approach for max-cut. *Computational Optimization and Applications*, 51:323–344, 01 2012. doi:[10.1007/s10589-010-9335-5](https://doi.org/10.1007/s10589-010-9335-5).
- [22] Martin Grötschel and George Nemhauser. A polynomial algorithm for the max-cut problem on graphs without long odd cycles. *Mathematical Programming*, 29(1):28 – 40, 1984.
- [23] Francisco Barahona and Ali Mahjoub. On the cut polytope. *Mathematical Programming*, 36:157–173, 06 1986. doi:[10.1007/BF02592023](https://doi.org/10.1007/BF02592023).
- [24] Michel Deza and Monique Laurent. *Geometry of Cuts and Metrics*. Springer, 1997.

- [25] Francisco Barahona, Michael Jünger, and Gerhard Reinelt. Experiments in quadratic 0–1 programming. *Mathematical Programming, Series A*, 44:127–137, 01 1989. doi:10.1007/BF01587084.
- [26] Michael Jünger and Sven Mallach. Odd-Cycle Separation for Maximum Cut and Binary Quadratic Optimization. In Michael A. Bender, Ola Svensson, and Grzegorz Herman, editors, *27th Annual European Symposium on Algorithms (ESA 2019)*, volume 144 of *Leibniz International Proceedings in Informatics (LIPIcs)*, pages 63:1–63:13, Dagstuhl, Germany, 2019. Schloss Dagstuhl–Leibniz-Zentrum fuer Informatik. doi:10.4230/LIPIcs.ESA.2019.63.
- [27] Michael Jünger and Sven Mallach. Exact facetial odd-cycle separation for maximum cut and binary quadratic optimization. *INFORMS Journal on Computing*, 33(4):1419–1430, 2021. arXiv:https://doi.org/10.1287/ijoc.2020.1008, doi:10.1287/ijoc.2020.1008.
- [28] David Avis and Jun Umemoto. Stronger linear programming relaxations of max-cut. *Mathematical Programming*, 97(3):451–469, Aug 2003. doi:10.1007/s10107-003-0423-5.
- [29] Wenceslas Fernandez de la Vega and Claire Kenyon-Mathieu. Linear programming relaxations of maxcut. In *Proceedings of the Eighteenth Annual ACM-SIAM Symposium on Discrete Algorithms*, SODA '07, page 53–61, USA, 2007. Society for Industrial and Applied Mathematics.
- [30] Daniel Rehfeldt, Thorsten Koch, and Yuji Shinano. Faster exact solution of sparse maxcut and qubo problems, 2022. doi:10.48550/ARXIV.2202.02305.
- [31] Jonas Charfreitag, Michael Jünger, Sven Mallach, and Petra Mutzel. Mcsparse: Exact solutions of sparse maximum cut and sparse unconstrained binary quadratic optimization problems. In *2022 Proceedings of the Symposium on Algorithm Engineering and Experiments (ALENEX)*, pages 54–66. SIAM, 2022. doi:10.1137/1.9781611977042.5.
- [32] Michel X. Goemans and David P. Williamson. Improved approximation algorithms for maximum cut and satisfiability problems using semidefinite programming. *J. ACM*, 42(6):1115–1145, nov 1995. doi:10.1145/227683.227684.
- [33] Subhash Khot, Guy Kindler, Elchanan Mossel, and Ryan O’Donnell. Optimal inapproximability results for max-cut and other 2-variable csps? *SIAM Journal on Computing*, 37(1):319–357, 2007. arXiv:https://doi.org/10.1137/S0097539705447372, doi:10.1137/S0097539705447372.
- [34] Uriel Feige and Gideon Schechtman. On the optimality of the random hyperplane rounding technique for max cut. *Random Structures & Algorithms*, 20(3):403–440, 2002. arXiv:https://onlinelibrary.wiley.com/doi/pdf/10.1002/rsa.10036, doi:10.1002/rsa.10036.
- [35] Franz Rendl, Giovanni Rinaldi, and Angelika Wiegele. A branch and bound algorithm for max-cut based on combining semidefinite and polyhedral relaxations. In Matteo Fischetti and David P. Williamson, editors, *Integer Programming and Combinatorial Optimization*, pages 295–309, Berlin, Heidelberg, 2007. Springer Berlin Heidelberg.
- [36] Franz Rendl, Giovanni Rinaldi, and Angelika Wiegele. Solving max-cut to optimality by intersecting semidefinite and polyhedral relaxations. *Mathematical Programming*, 121(2):307–335, Feb 2010. doi:10.1007/s10107-008-0235-8.
- [37] Laura Palagi, Veronica Piccialli, Franz Rendl, Giovanni Rinaldi, and Angelika Wiegele. *Computational Approaches to Max-Cut*, pages 821–847. Springer US, New York, NY, 2012. doi:10.1007/978-1-4614-0769-0_28.
- [38] Christoph Buchheim, Frauke Liers, and Marcus Oswald. Speeding up ip-based algorithms for constrained quadratic 0–1 optimization. *Mathematical Programming*, 124(1):513–535, Jul 2010. doi:10.1007/s10107-010-0377-3.

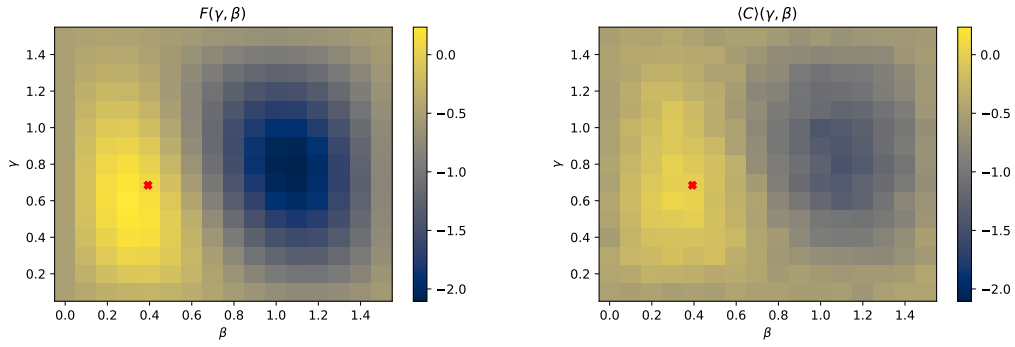
- [39] Frank Arute, Kunal Arya, Ryan Babbush, Dave Bacon, Joseph C. Bardin, Rami Barends, Rupak Biswas, Sergio Boixo, Fernando G. S. L. Brandao, David A. Buell, Brian Burkett, Yu Chen, Zijun Chen, Ben Chiaro, Roberto Collins, William Courtney, Andrew Dunsworth, Edward Farhi, Brooks Foxen, Austin Fowler, Craig Gidney, Marissa Giustina, Rob Graff, Keith Guerin, Steve Habegger, Matthew P. Harrigan, Michael J. Hartmann, Alan Ho, Markus Hoffmann, Trent Huang, Travis S. Humble, Sergei V. Isakov, Evan Jeffrey, Zhang Jiang, Dvir Kafri, Kostyantyn Kechedzhi, Julian Kelly, Paul V. Klimov, Sergey Knysh, Alexander Korotkov, Fedor Kostritsa, David Landhuis, Mike Lindmark, Erik Lucero, Dmitry Lyakh, Salvatore Mandrà, Jarrod R. McClean, Matthew McEwen, Anthony Megrant, Xiao Mi, Kristel Michielsen, Masoud Mohseni, Josh Mutus, Ofer Naaman, Matthew Neeley, Charles Neill, Murphy Yuezhen Niu, Eric Ostby, Andre Petukhov, John C. Platt, Chris Quintana, Eleanor G. Rieffel, Pedram Roushan, Nicholas C. Rubin, Daniel Sank, Kevin J. Satzinger, Vadim Smelyanskiy, Kevin J. Sung, Matthew D. Trevithick, Amit Vainsencher, Benjamin Villalonga, Theodore White, Z. Jamie Yao, Ping Yeh, Adam Zalcman, Hartmut Neven, and John M. Martinis. Quantum supremacy using a programmable superconducting processor. *Nature*, 574(7779):505–510, Oct 2019. doi:10.1038/s41586-019-1666-5.
- [40] Eric Hyyppä, Suman Kundu, Chun Fai Chan, András Gulyás, Juho Hotari, David Janzso, Kristinn Juliusson, Olavi Kiuru, Janne Kotilahti, Alessandro Landra, Wei Liu, Fabian Marxer, Akseli Mäkinen, Jean-Luc Orgiazzi, Mario Palma, Mykhailo Savytskyi, Francesca Tosto, Jani Tuorila, Vasili Vadimov, Tianyi Li, Caspar Ockeloen-Korppi, Johannes Heinsoo, Kuan Yen Tan, Juha Hassel, and Mikko Möttönen. Unimon qubit. *Nature Communications*, 13(1), nov 2022. doi:10.1038/s41467-022-34614-w.
- [41] Philipp Hauke, Helmut G Katzgraber, Wolfgang Lechner, Hidetoshi Nishimori, and William D Oliver. Perspectives of quantum annealing: methods and implementations. *Reports on Progress in Physics*, 83(5):054401, may 2020. doi:10.1088/1361-6633/ab85b8.
- [42] Kelly Boothby, Colin Enderud, Trevor Lanting, Reza Molavi, Nicholas Tsai, Mark H. Volkmann, Fabio Altomare, Mohammad H. Amin, Michael Babcock, Andrew J. Berkley, Catia Baron Aznar, Martin Boschnak, Holly Christiani, Sara Ejtemaee, Bram Evert, Matthew Gullen, Markus Hager, Richard Harris, Emile Hoskinson, Jeremy P. Hilton, Kais Jooya, Ann Huang, Mark W. Johnson, Andrew D. King, Eric Ladizinsky, Ryan Li, Allison MacDonald, Teresa Medina Fernandez, Richard Neufeld, Mana Norouzpour, Travis Oh, Isil Ozfidan, Paul Paddon, Ilya Perminov, Gabriel Poulin-Lamarre, Thomas Prescott, Jack Raymond, Mauricio Reis, Chris Rich, Aidan Roy, Hossein Sadeghi Esfahani, Yuki Sato, Ben Sheldan, Anatoly Smirnov, Loren J. Swenson, Jed Whittaker, Jason Yao, Alexander Yarovoy, and Paul I. Bunyk. Architectural considerations in the design of a third-generation superconducting quantum annealing processor, 2021. arXiv:2108.02322.
- [43] Troels F. Rønnow, Zhihui Wang, Joshua Job, Sergio Boixo, Sergei V. Isakov, David Wecker, John M. Martinis, Daniel A. Lidar, and Matthias Troyer. Defining and detecting quantum speedup. *Science*, 345(6195):420–424, 2014. arXiv:https://www.science.org/doi/pdf/10.1126/science.1252319, doi:10.1126/science.1252319.
- [44] Peter L. Ivănescu. Some network flow problems solved with pseudo-boolean programming. *Operations Research*, 13(3):388–399, 1965. arXiv:https://doi.org/10.1287/opre.13.3.388, doi:10.1287/opre.13.3.388.
- [45] Caterina De Simone. The cut polytope and the boolean quadric polytope. *Discrete Mathematics*, 79(1):71–75, 1990. doi:10.1016/0012-365X(90)90056-N.
- [46] Andrew Lucas. Ising formulations of many NP problems. *Frontiers in Physics*, 2, 2014. doi:10.3389/fphy.2014.00005.
- [47] Vicky Siu-Ngan Choi. Minor-embedding in adiabatic quantum computation: I. the parameter setting problem. *Quantum Information Processing*, 7:193–209, 2008. doi:10.1007/s11128-008-0082-9.

- [48] Vicky Choi. Minor-embedding in adiabatic quantum computation: II. minor-universal graph design. *Quantum Information Processing*, 10(3):343–353, October 2010. doi:[10.1007/s11128-010-0200-3](https://doi.org/10.1007/s11128-010-0200-3).
- [49] Friedrich Wagner, Andreas Bärman, Frauke Liers, and Markus Weissenböck. Improving quantum computation by optimized qubit routing. *Journal of Optimization Theory and Applications*, 197(3):1161–1194, may 2023. doi:[10.1007/s10957-023-02229-w](https://doi.org/10.1007/s10957-023-02229-w).
- [50] Michael A. Nielsen and Isaac L. Chuang. *Quantum Computation and Quantum Information: 10th Anniversary Edition*. Cambridge University Press, 2010. doi:[10.1017/CBO9780511976667](https://doi.org/10.1017/CBO9780511976667).
- [51] Ewout van den Berg, Zlatko K. Mineev, and Kristan Temme. Model-free readout-error mitigation for quantum expectation values. *Physical Review A*, 105(3), mar 2022. doi:[10.1103/physreva.105.032620](https://doi.org/10.1103/physreva.105.032620).
- [52] Kristan Temme, Sergey Bravyi, and Jay M. Gambetta. Error mitigation for short-depth quantum circuits. *Physical Review Letters*, 119(18), nov 2017. doi:[10.1103/physrevlett.119.180509](https://doi.org/10.1103/physrevlett.119.180509).
- [53] Sergey Bravyi, Alexander Kliesch, Robert Koenig, and Eugene Tang. Obstacles to variational quantum optimization from symmetry protection. *Physical Review Letters*, 125(26), dec 2020. doi:[10.1103/physrevlett.125.260505](https://doi.org/10.1103/physrevlett.125.260505).
- [54] Edward Farhi, Jeffrey Goldstone, Sam Gutmann, and Leo Zhou. The quantum approximate optimization algorithm and the sherrington-kirkpatrick model at infinite size. *Quantum*, 6:759, July 2022. doi:[10.22331/q-2022-07-07-759](https://doi.org/10.22331/q-2022-07-07-759).
- [55] Joao Basso, Edward Farhi, Kunal Marwaha, Benjamin Villalonga, and Leo Zhou. The quantum approximate optimization algorithm at high depth for maxcut on large-girth regular graphs and the sherrington-kirkpatrick model. Schloss Dagstuhl – Leibniz-Zentrum für Informatik, 2022. doi:[10.4230/LIPICS.TQC.2022.7](https://doi.org/10.4230/LIPICS.TQC.2022.7).
- [56] Zhihui Wang, Stuart Hadfield, Zhang Jiang, and Eleanor G. Rieffel. Quantum approximate optimization algorithm for MaxCut: A fermionic view. *Physical Review A*, 97(2), feb 2018. doi:[10.1103/physreva.97.022304](https://doi.org/10.1103/physreva.97.022304).
- [57] Asier Ozaeta, Wim van Dam, and Peter L McMahon. Expectation values from the single-layer quantum approximate optimization algorithm on ising problems. *Quantum Science and Technology*, 7(4):045036, September 2022. doi:[10.1088/2058-9565/ac9013](https://doi.org/10.1088/2058-9565/ac9013).
- [58] Sergey Bravyi, Alexander Kliesch, Robert Koenig, and Eugene Tang. Hybrid quantum-classical algorithms for approximate graph coloring. *Quantum*, 6:678, March 2022. URL: <http://dx.doi.org/10.22331/q-2022-03-30-678>, doi:[10.22331/q-2022-03-30-678](https://doi.org/10.22331/q-2022-03-30-678).
- [59] Jernej Rudi Finžgar, Aron Kerschbaumer, Martin J. A. Schuetz, Christian B. Mendl, and Helmut G. Katzgraber. Quantum-informed recursive optimization algorithms, 2023. arXiv: [2308.13607](https://arxiv.org/abs/2308.13607).
- [60] Maxime Dupont and Bhuvanesh Sundar. Extending relax-and-round combinatorial optimization solvers with quantum correlations. *Physical Review A*, 109(1), January 2024. doi:[10.1103/physreva.109.012429](https://doi.org/10.1103/physreva.109.012429).
- [61] Reuben Tate, Majid Farhadi, Creston Herold, Greg Mohler, and Swati Gupta. Bridging classical and quantum with sdp initialized warm-starts for qaoa. *ACM Transactions on Quantum Computing*, 4(2), feb 2023. doi:[10.1145/3549554](https://doi.org/10.1145/3549554).
- [62] Daniel J. Egger, Jakub Mareček, and Stefan Woerner. Warm-starting quantum optimization. *Quantum*, 5:479, June 2021. doi:[10.22331/q-2021-06-17-479](https://doi.org/10.22331/q-2021-06-17-479).

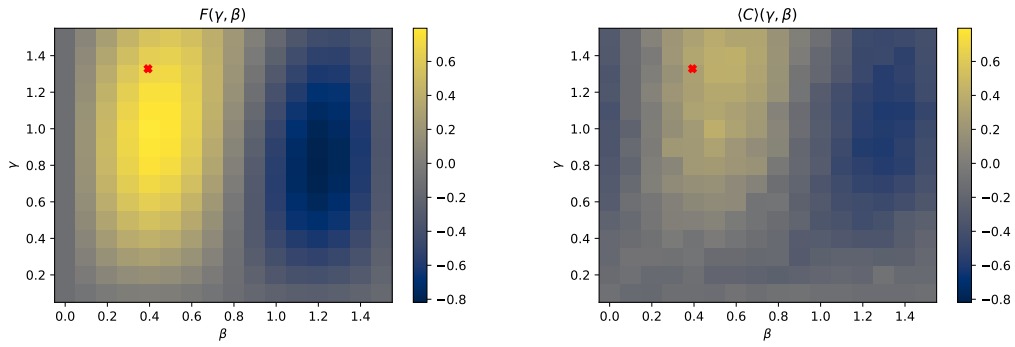
- [63] Jack Raymond, Radomir Stevanovic, William Bernoudy, Kelly Boothby, Catherine C. McGeoch, Andrew J. Berkley, Pau Farré, Joel Pasvolsky, and Andrew D. King. Hybrid quantum annealing for larger-than-qpu lattice-structured problems. *ACM Transactions on Quantum Computing*, 4(3), apr 2023. doi:10.1145/3579368.
- [64] Stuart Hadfield. Quantum algorithms for scientific computing and approximate optimization, 2018. arXiv:1805.03265.
- [65] Ruslan Shaydulin, Phillip C. Lotshaw, Jeffrey Larson, James Ostrowski, and Travis S. Humble. Parameter transfer for quantum approximate optimization of weighted maxcut. *ACM Transactions on Quantum Computing*, 4(3), apr 2023. doi:10.1145/3584706.
- [66] Jan-Hendrik Lange, Bjoern Andres, and Paul Swoboda. Combinatorial persistency criteria for multicut and max-cut, 2018. doi:10.48550/ARXIV.1812.01426.
- [67] Damir Ferizovic, Demian Hespe, Sebastian Lamm, Matthias Mnich, Christian Schulz, and Darren Strash. Engineering kernelization for maximum cut. In *2020 Proceedings of the Workshop on Algorithm Engineering and Experiments (ALENEX), Salt Lake City, Utah, U.S., January 5 - 6, 2020. Ed.: G. Blelloch*, page 27–41. Society for Industrial and Applied Mathematics (SIAM), 2020. 46.12.02; LK 01. doi:10.1137/1.9781611976007.3.
- [68] Frauke Liers and G. Pardella. Simplifying maximum flow computations: The effect of shrinking and good initial flows. *Discrete Applied Mathematics*, 159:2187–2203, 10 2011. doi:10.1016/j.dam.2011.06.030.
- [69] Stuart Hadfield, Zihui Wang, Bryan O’Gorman, Eleanor G. Rieffel, Davide Venturelli, and Rupak Biswas. From the quantum approximate optimization algorithm to a quantum alternating operator ansatz. *Algorithms*, 12(2), 2019. doi:10.3390/a12020034.
- [70] Qiskit. An open-source framework for quantum computing. <http://www.qiskit.org>, 2021. doi:10.5281/zenodo.2573505.
- [71] Aric A. Hagberg, Daniel A. Schult, and Pieter J. Swart. Exploring network structure, dynamics, and function using networkx. In Gaël Varoquaux, Travis Vaught, and Jarrod Millman, editors, *Proceedings of the 7th Python in Science Conference*, pages 11 – 15, Pasadena, CA USA, 2008.
- [72] Gurobi Optimization, LLC. Gurobi Optimizer Reference Manual, 2023. URL: <https://www.gurobi.com>.
- [73] IBM Quantum. <https://quantum-computing.ibm.com/>, 2021.
- [74] Leo Zhou, Sheng-Tao Wang, Soonwon Choi, Hannes Pichler, and Mikhail D. Lukin. Quantum approximate optimization algorithm: Performance, mechanism, and implementation on near-term devices. *Physical Review X*, 10(2), jun 2020. doi:10.1103/physrevx.10.021067.
- [75] Don Coppersmith, David Gamarnik, MohammadTaghi Hajiaghayi, and Gregory B. Sorkin. Random max sat, random max cut, and their phase transitions. *Random Structures & Algorithms*, 24(4):502–545, 2004.
- [76] Angelika Wiegele. Biq mac library – binary quadratic and max cut library, 2007. URL: <https://biqmac.aau.at/biqmaclib.html>.

A Additional Figures

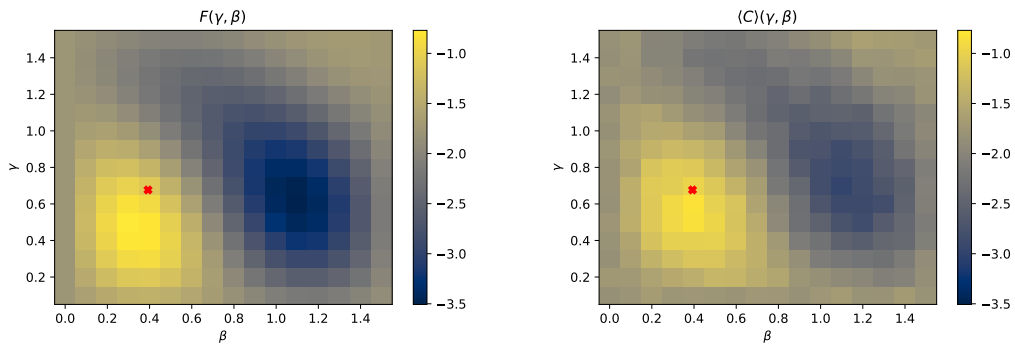
A.1 Parameter Estimate Evaluation



(a) Instance d.



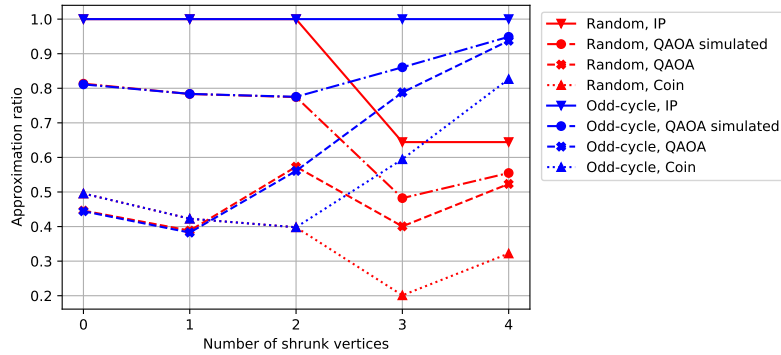
(b) Instance e.



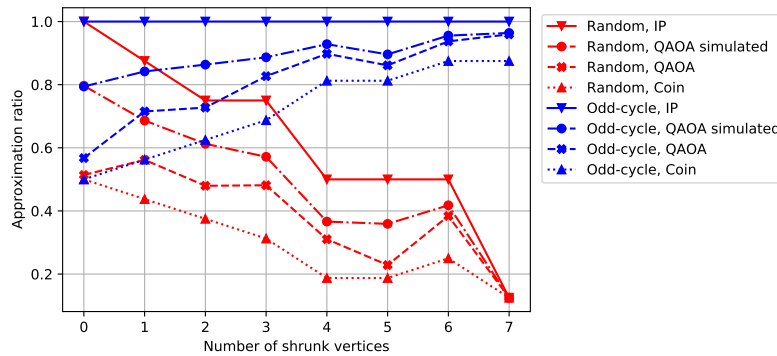
(c) Instance f.

Figure 7: Visualized results for QAOA parameter-estimate on instances d, e and f from Fig. 3. Compare Fig. 4.

A.2 Combining Shrinking with QAOA



(a) Instance k6n from Table 2.



(b) Instance 3x3b from Table 2.

Figure 8: Further results for evaluating the shrinking-algorithm with different setting. Compare Fig. 5.

Acknowledgements

This research has been supported by the Bavarian Ministry of Economic Affairs, Regional Development and Energy with funds from the Hightech Agenda Bayern and by the Federal Ministry for Economic Affairs and Climate Action on the basis of a decision by the German Bundestag through project QuaST.